Supplementary Information

Diastereomerically-Differentiated Excited State Behavior in Ruthenium(II) Hexafluoroacetylacetonate Complexes of Diphenyl Thioindigo Diimine

Geneviève N. Boice,† Sofia Garakyaraghi,‡ Brian O. Patrick,§ Corey Sanz,† Felix N. Castellano,‡* Robin G. Hicks†*

† Department of Chemistry, University of Victoria, PO Box 3065 STN CSC, Victoria, BC V8W 3V6, Canada

‡ Department of Chemistry, North Carolina State University, Raleigh, North Carolina, 27695-8204, United States of America

§ Crystallography Laboratory, Department of Chemistry, University of British Columbia, Vancouver, BC, V6T 1Z1, Canada

Table of Contents

1. X-ray crystallographic data for compounds **1a–b** and **2** **S3**

2. Physical molecular models of compound **1a** and **1b** **S4**

3. Structural distribution of ^{1}H and ^{13}C atoms in compound **1b** that exhibit broadened peaks in room temperature NMR experiments **S5**

4. Solvatochromism of compounds **1b** and **2** **S5-S7**

5. Transient decay traces of compounds **1a-b** and **2** **S7-S9**

6. Low resolution mass spectra and matching to predicted isotope patterns for compounds **1a-b** and **2** **S10-S12**

7. ^{1}H, ^{19}F, ^{13}C, COSY, HSQC, HMBC NMR spectra for compound **1a** **S13-S21**

8. ^{1}H, ^{19}F, ^{13}C, COSY, HSQC, HMBC NMR spectra for compound **1b** **S22-S31**

9. ^{1}H, ^{19}F, ^{13}C NMR spectra for compound **2** **S32-S34**

10. Variable temperature ^{1}H NMR spectra of compound **1b**, winDNMR simulations, Eyring plots, and $\Delta G^{\ddagger}$ calculations **S34-S38**

11. Low temperature ^{19}F spectra for compound **1b** and low temperature ^{1}H NMR spectra for compound **1a** **S39-S41**

1. X-ray crystallographic data for compounds **1a–b** and **2**

Table S1. Crystallographic Data for Diruthenium Complexes **1a–b** and Monoruthenium Complex **2.**

	1a	**1b**	**2**
Empirical Formula	$C_{48}H_{22}F_{24}N_2O_8Ru_2S_2$	$C_{48}H_{22}F_{24}N_2O_8Ru_2S_2$	$C_{38}H_{20}F_{12}N_2O_4RuS_2$
Formula Weight	1476.93	1476.93	961.75
a (Å)	9.188(3)	29.613(6)	8.5769(7)
b (Å)	12.530(4)	9.667(2)	13.7143(14)
c (Å)	23.373(8)	37.632(8)	16.8117(16)
α (deg)	78.561(6)	90	66.471(5)
β (deg)	87.404(7)	98.402 (4)	89.755(4)
γ (deg)	87.711(6)	90	88.118(5)
V (Å^3)	2633.4(15)	10657(4)	1812.0(3)
Z	2	16	2
space group	*P*-1	C2/c	*P* -1 (#2)
T (°C)	-183	-183	-173.0 ± 2
λ (Å)	0.71073	0.71073	0.71073
D_{calcd} (g cm^{-3})	1.863	1.841	1.763
μ (cm^{-1})	7.93	7.84	6.56
R [all data] [a]	0.0782	0.0667	0.066
R_w [all data] [b]	0.1541	0.1371	0.165
CCDC#	1548434	1548435	1548433

[a] $R = \sum|F_{obs}-F_{calc}|/\sum|F_{obs}|$. [b] $R_w = [\sum(|w||F_{obs}-F_{calc}|)^2/\sum|wF_{obs}^2|]^{1/2}$.

2. Physical models of compound **1a** and **1b** showing orientation of hfac ligands and phenyl rings

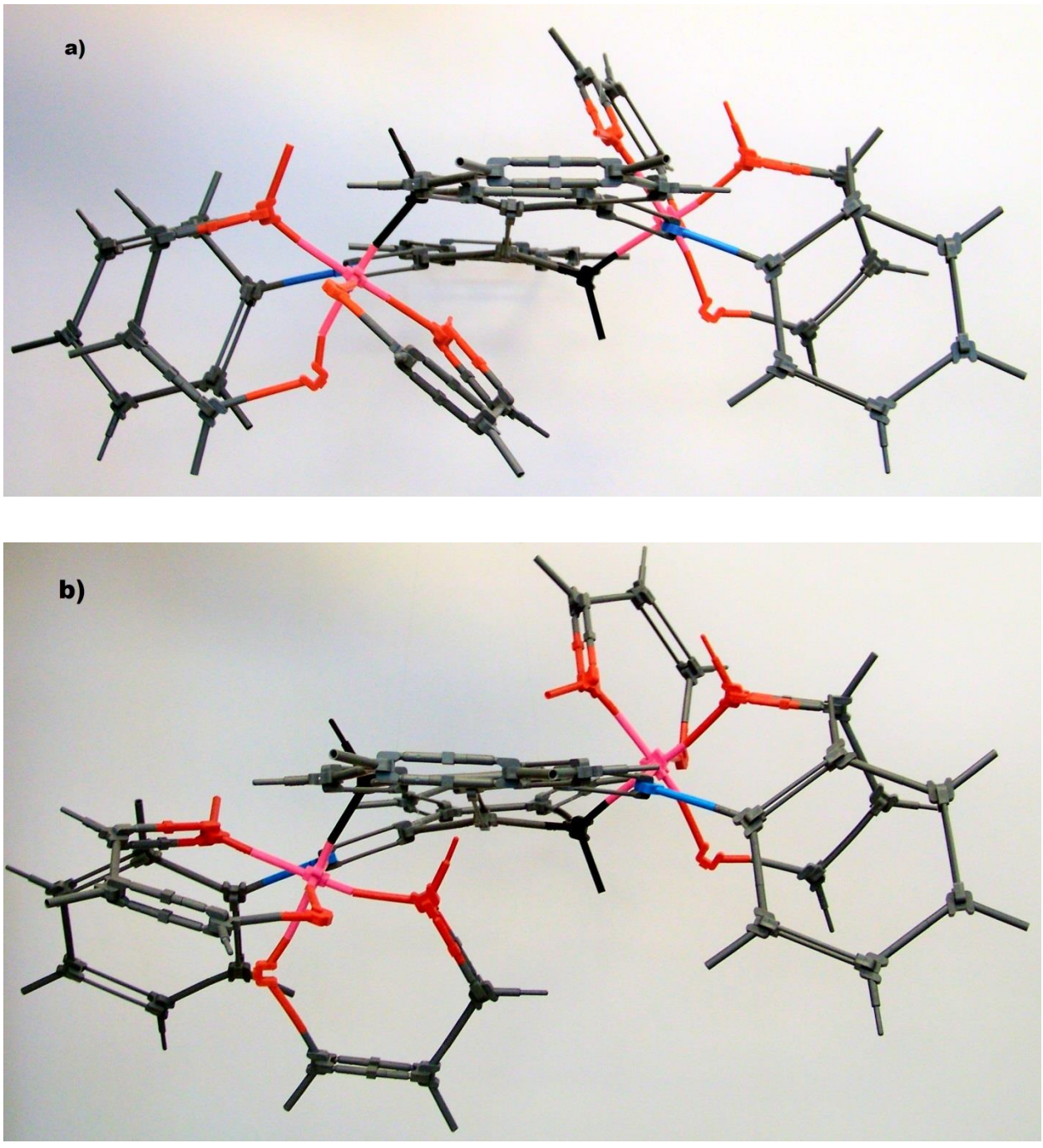

Figure S1. Physical molecular models of a) *meso* diruthenium complex **1a** and b) the ΔΔ enantiomer of *rac* diruthenium complex **1b**. The trifluoromethyl groups of the β-diketonate ligands have been removed for clarity.

3. Structural distribution of ^{1}H and ^{13}C atoms in compound **1b** that exhibit broadened peaks in room temperature NMR experiments.

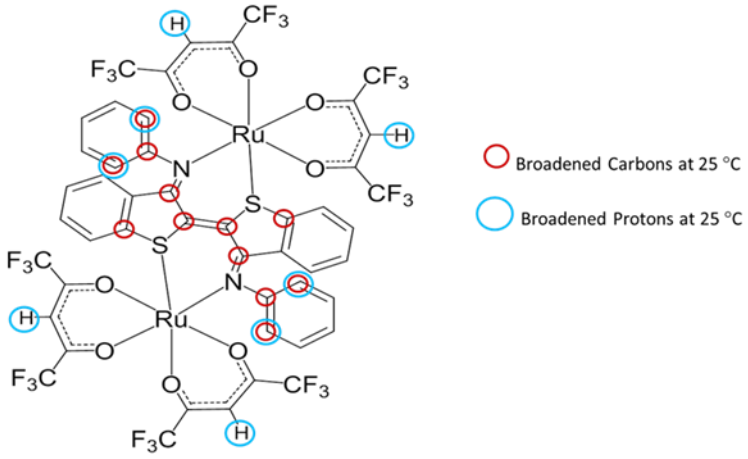

Figure S2. *Rac* diruthenium complex **1b**. Carbon atoms with broadened NMR signals at 25 ºC are circled in red. Hydrogen atoms (or the carbon to which they are bonded) with broadened NMR signals at 25 ºC are circled in blue.

4. Solvatochromism of compounds **1b** and **2**

Compounds **1b** and **2** were each dissolved in the following spectrograde solvents in micromolar concentrations: hexane, acetonitrile, toluene, tetrahydrofuran, and methanol. Spectra were collected under air atmosphere.

The shift observed for the MLCT (d to π*) band of compound **2** is 643 cm^{-1}.The absorption maximum blue-shifts with increasing solvent polarity. No clear trend emerges for the (proposed) π to π* band in the same compound.

A blue-shift is observed for the MLCT (d to π*) band of diruthenium compound **1b** in solvents of increasing polarity. The change in absorption maximum is 453 cm^{-1}. No clear trend emerges for the (proposed) π to π* band in the same compound.

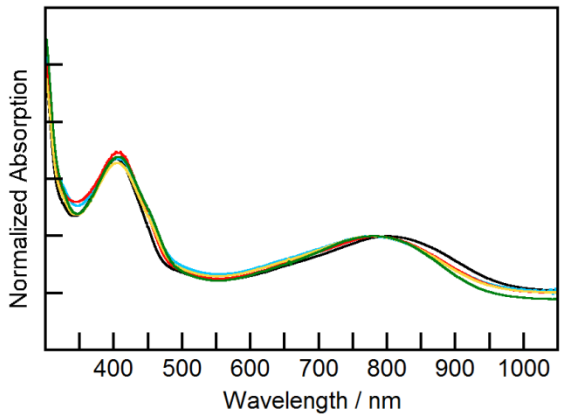

Figure S3. Normalized absorption spectrum of *rac*-diruthenium complex **1b** in solvents, from right to left: hexanes (black), toluene (red), tetrahydrofuran (blue), methanol (yellow), acetonitrile (green).

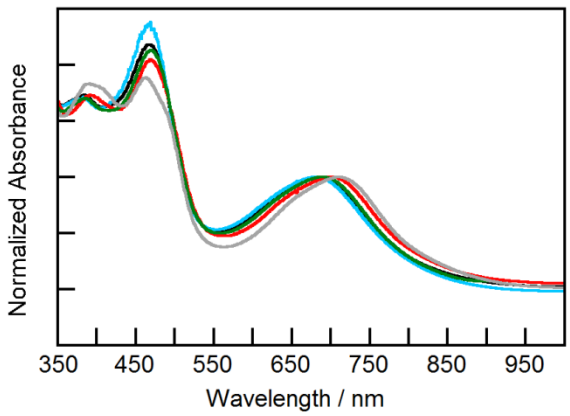

Figure S3. Normalized absorption spectrum of monoruthenium complex **2** in solvents, from right to left: hexanes (grey), toluene (red), tetrahydrofuran (green), methanol (black), acetonitrile (blue).

Table S2. Absorbance maxima of compounds 1b and 2 in solvent of varying polarity.

Solvent	Monoruthenium **2**				Diruthenium **1b**			
	λ_{max1}^{abs}		λ_{max2}^{abs}		λ_{max1}^{abs}		λ_{max2}^{abs}	
	/ nm	/ cm^{-1}	/ nm	/ cm^{-1}	/ nm	/ cm^{-1}	/ nm	/ cm^{-1}
Acetonitrile	679	14728	468	21368	775	12903	405	24691
Methanol	683	14641	465	21505	774	12920	405	24691
Tetrahydrofuran	689	14514	469	21322	773	12937	406	24630
Toluene	698	14327	469	21322	785	12739	403	24814
Hexane	710	14085	463	21598	801	12484	404	24753

5. Transient absorption kinetics of compounds **1a-b** and **2**

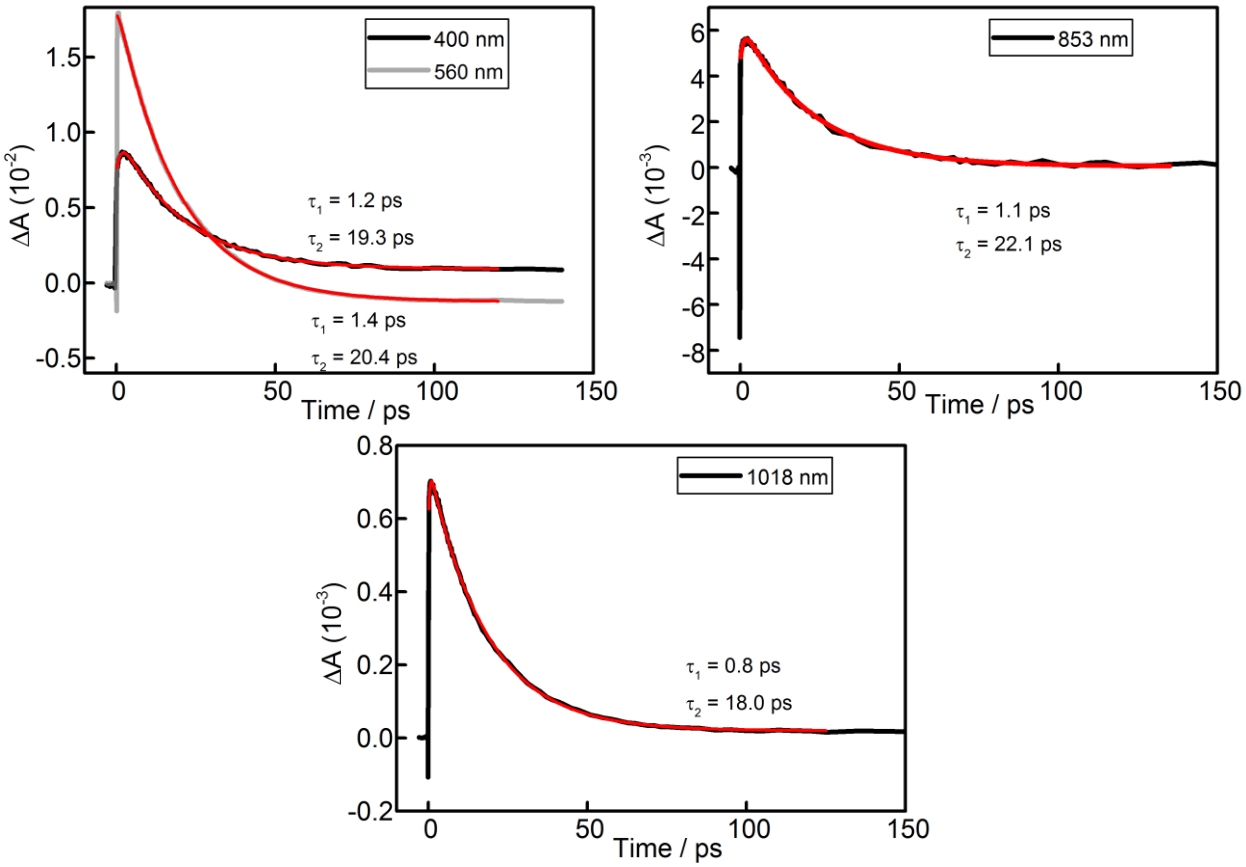

Figure S5. Transient decay traces of monoruthenium complex **2**. The λ_{ex} is 700 nm. The pulse power is 0.5 µJ. The monitoring wavelengths and extracted rate constants are indicated in the graphs.

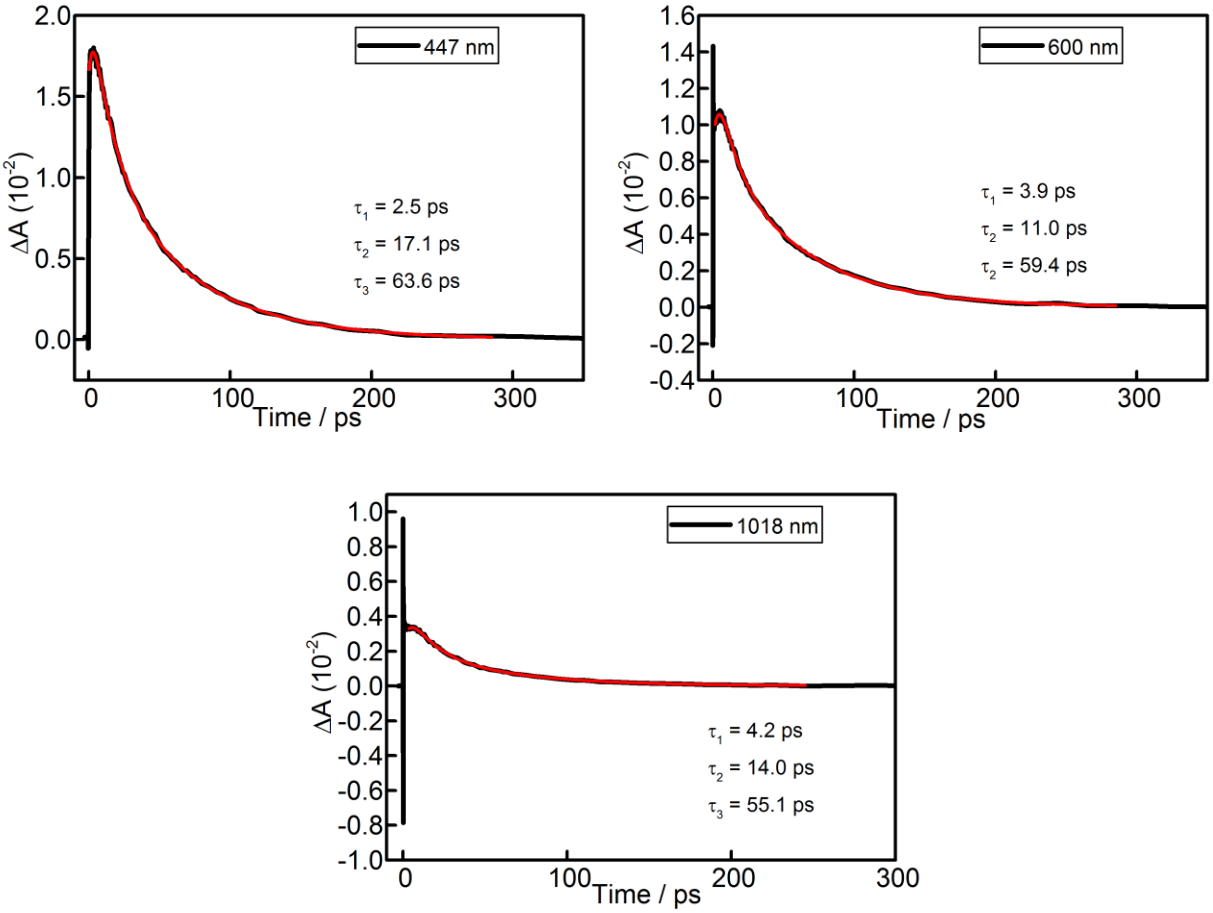

Figure S6. Transient decay traces of *meso* diruthenium complex **1a**. The λ_{ex} is 800 nm and the pulse power is 1.0 μJ. The monitoring wavelengths and extracted rate constants are indicated in the graphs.

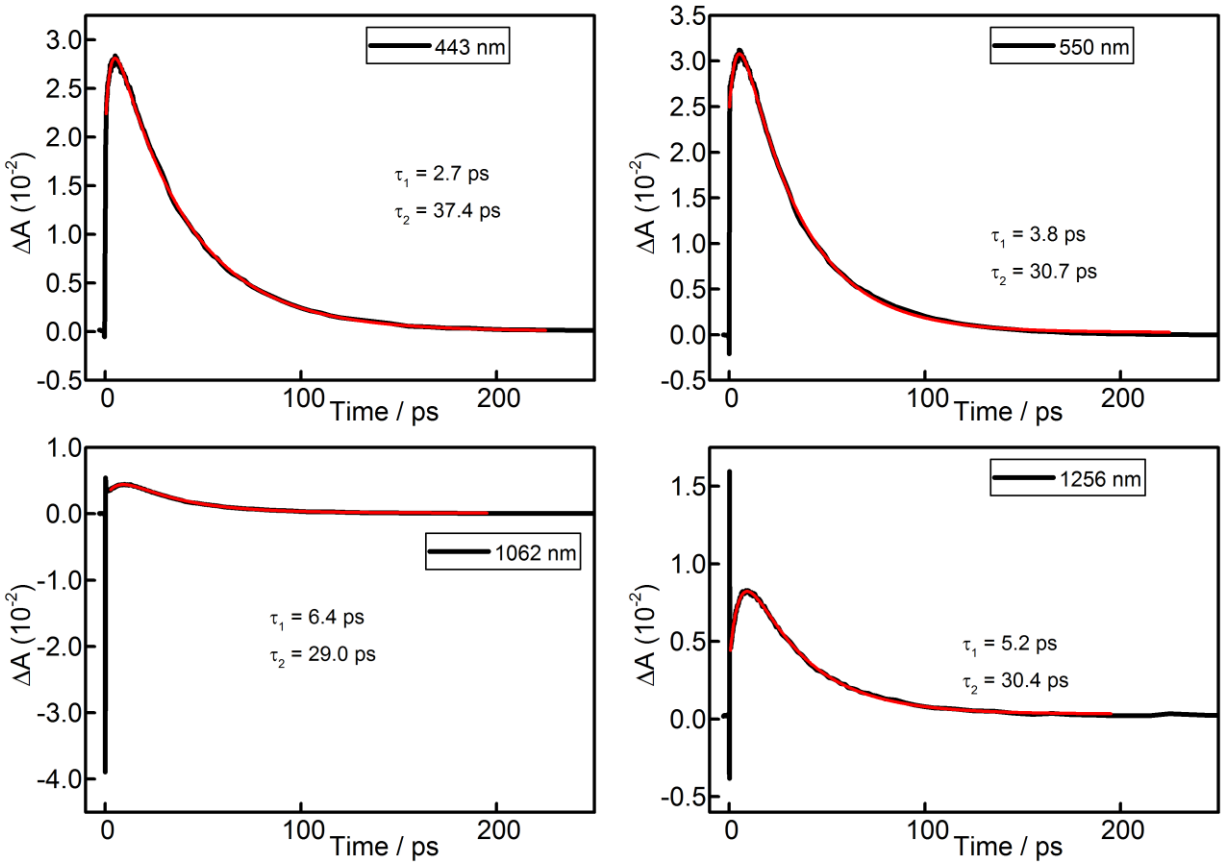

Figure S7. Transient decay traces of *rac* diruthenium complex **1b**. The λ_{ex} is 800 nm. The pulse power is 1.5 μJ in the 443 and 550 nm traces; it is 1.0 μJ in the 1062 and 1256 traces). The monitoring wavelengths and extracted rate constants are indicated in the graphs.

6. Low resolution mass spectra and matching to predicted isotope patterns for compounds **1a-b** and **2**

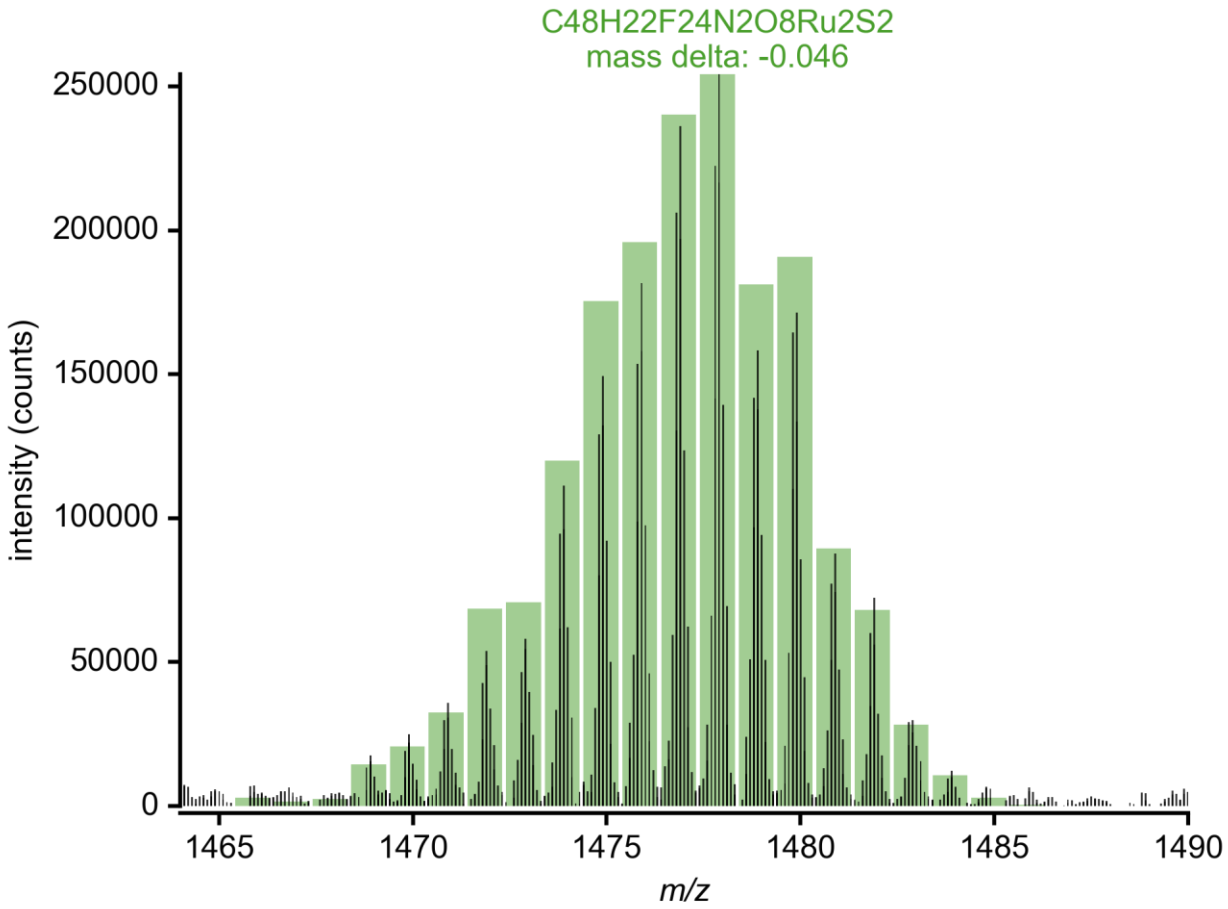

Figure S8. Mass spectrum of *meso* diruthenium complex **1a** with overlay of predicted isotope pattern for M+.

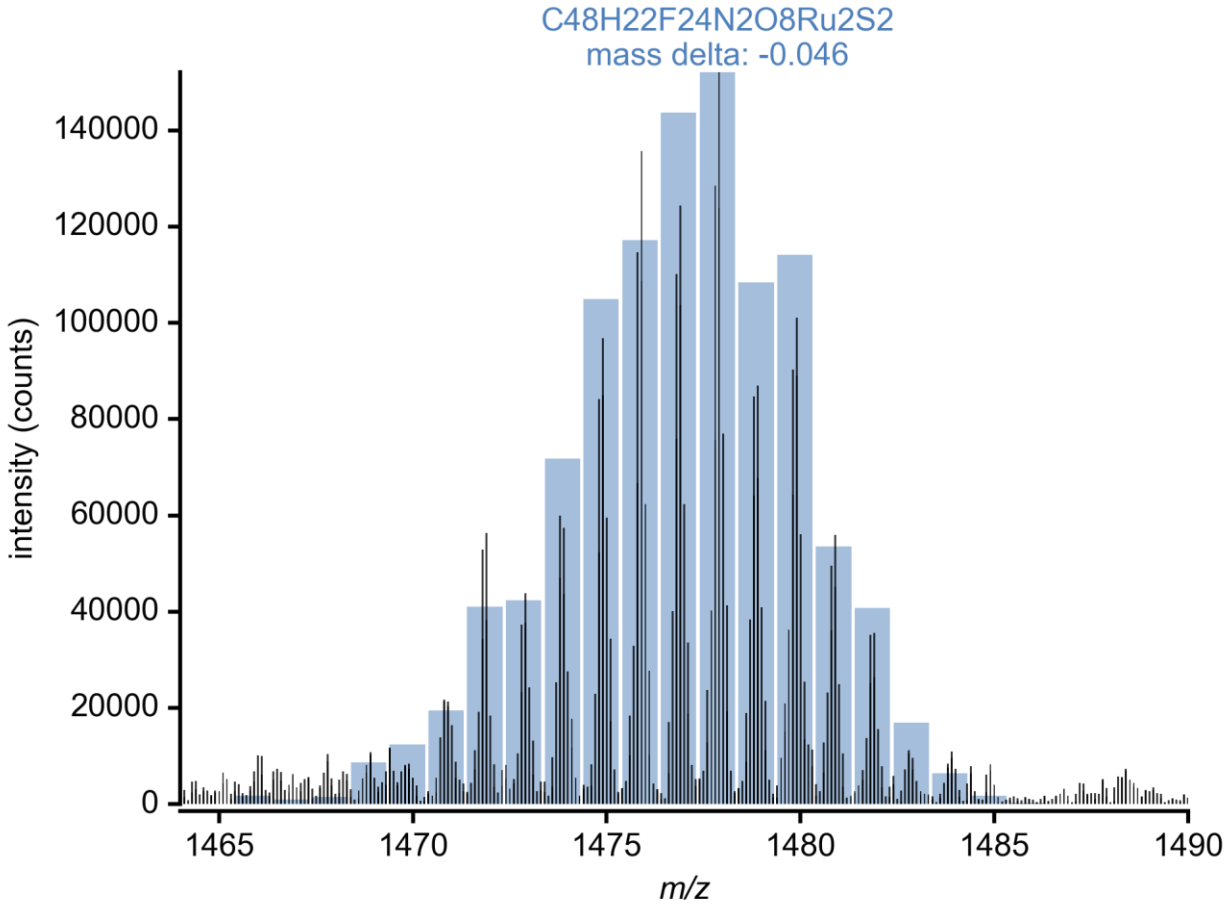

Figure S9. Mass spectrum of *rac* diruthenium complex **1b** with overlay of predicted isotope pattern for M+.

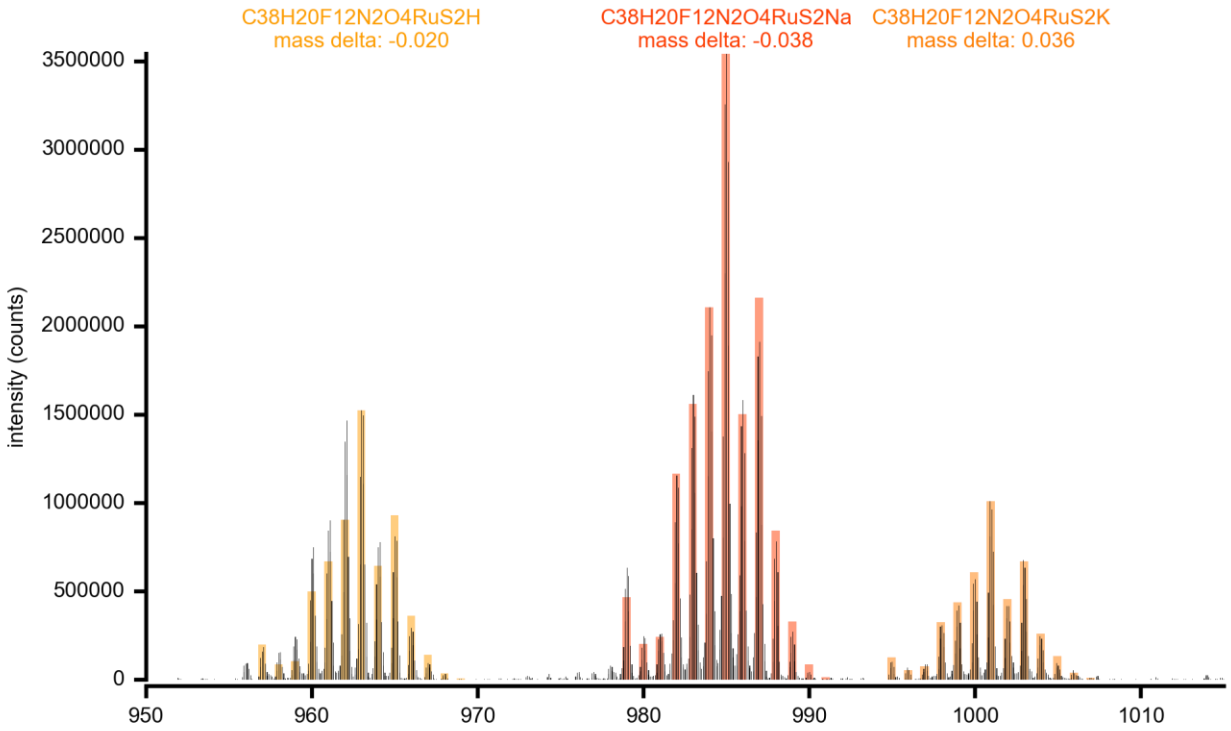

Figure S10. Mass spectrum of monoRuthenium complex **2** with overlay of predicted isotope pattern for M+H (left), M+Na (middle), and M+K (right).

7. ^{1}H, ^{19}F, ^{13}C, COSY, HSQC, HMBC NMR spectra for compound **1a**

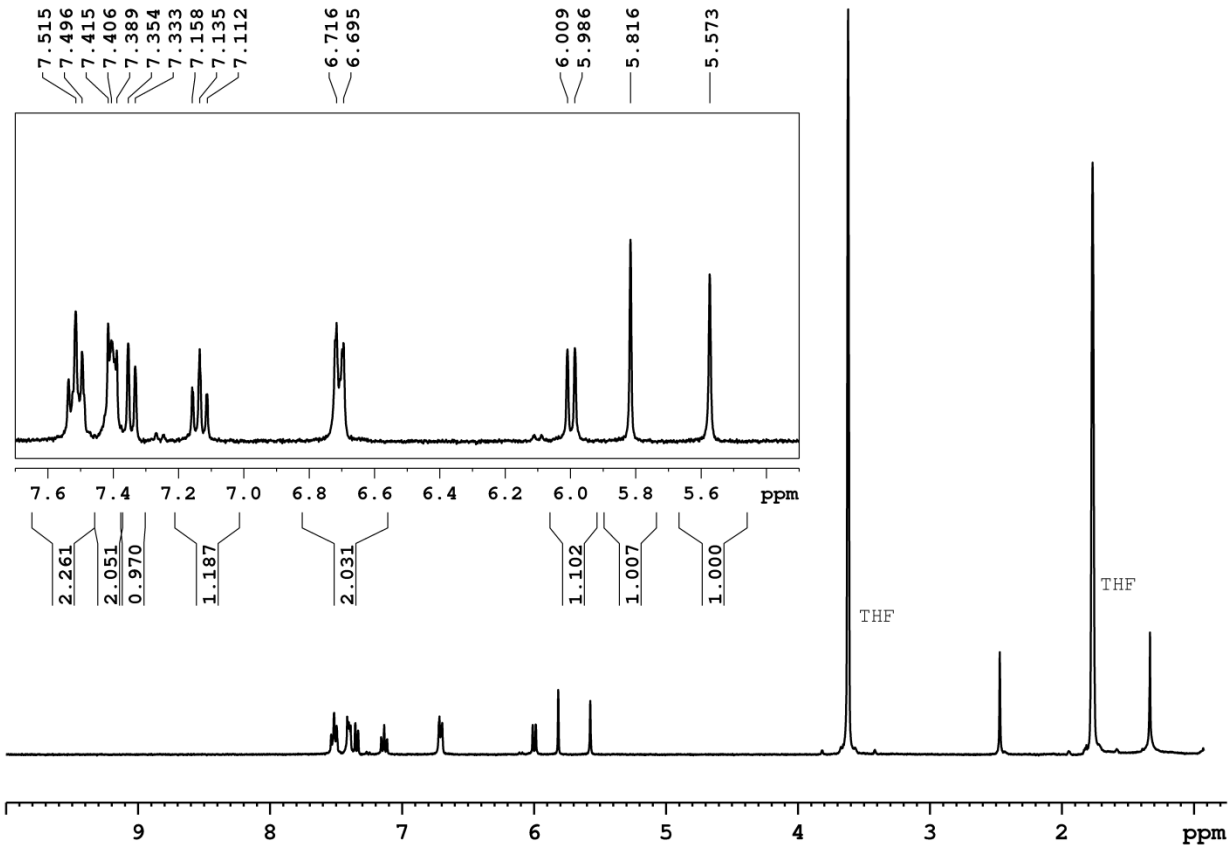

Figure S11. ^{1}H NMR (360 MHz, *d8*-THF, 298 K) spectrum of *meso* diruthenium complex **1a**.

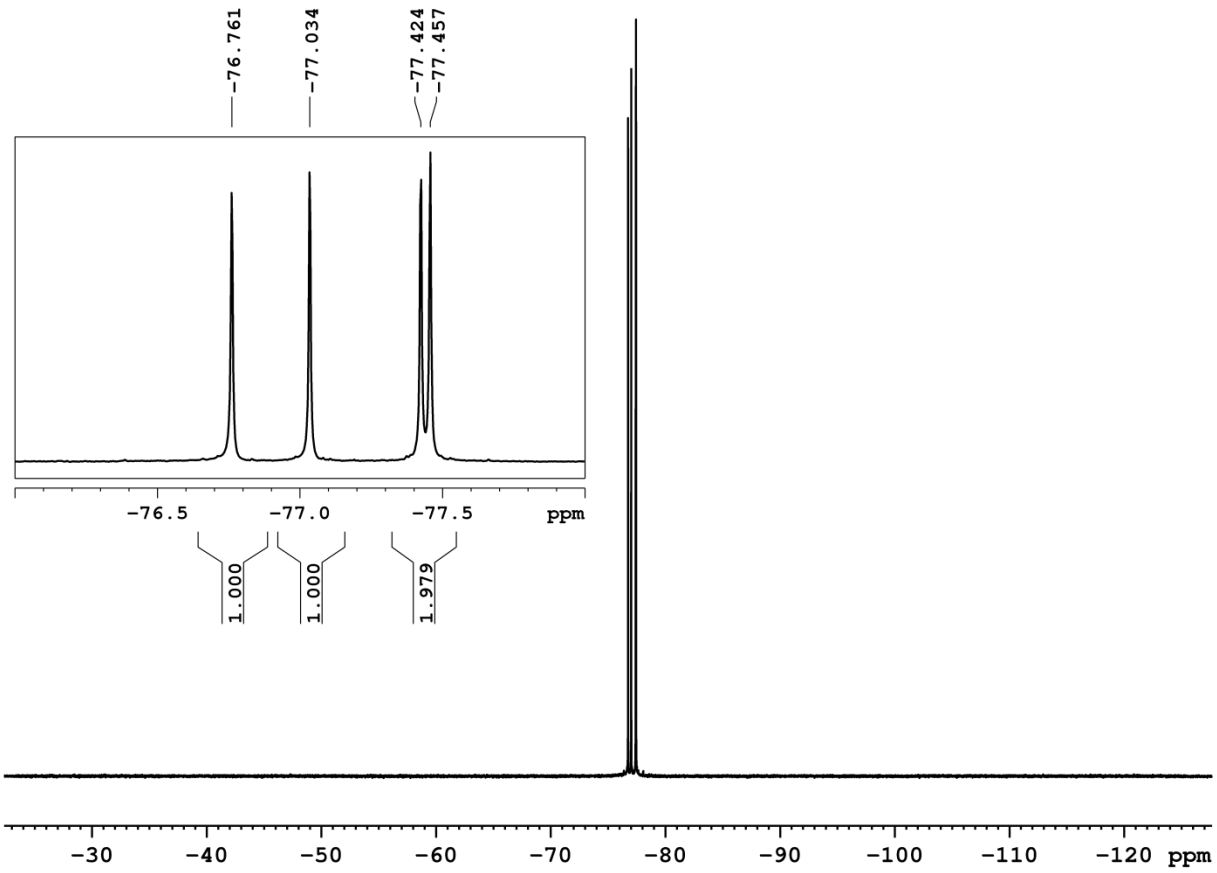

Figure S12. ^{19}F NMR (282 MHz, *d8*-THF, 298 K) spectrum of *meso* diruthenium complex **1a**.

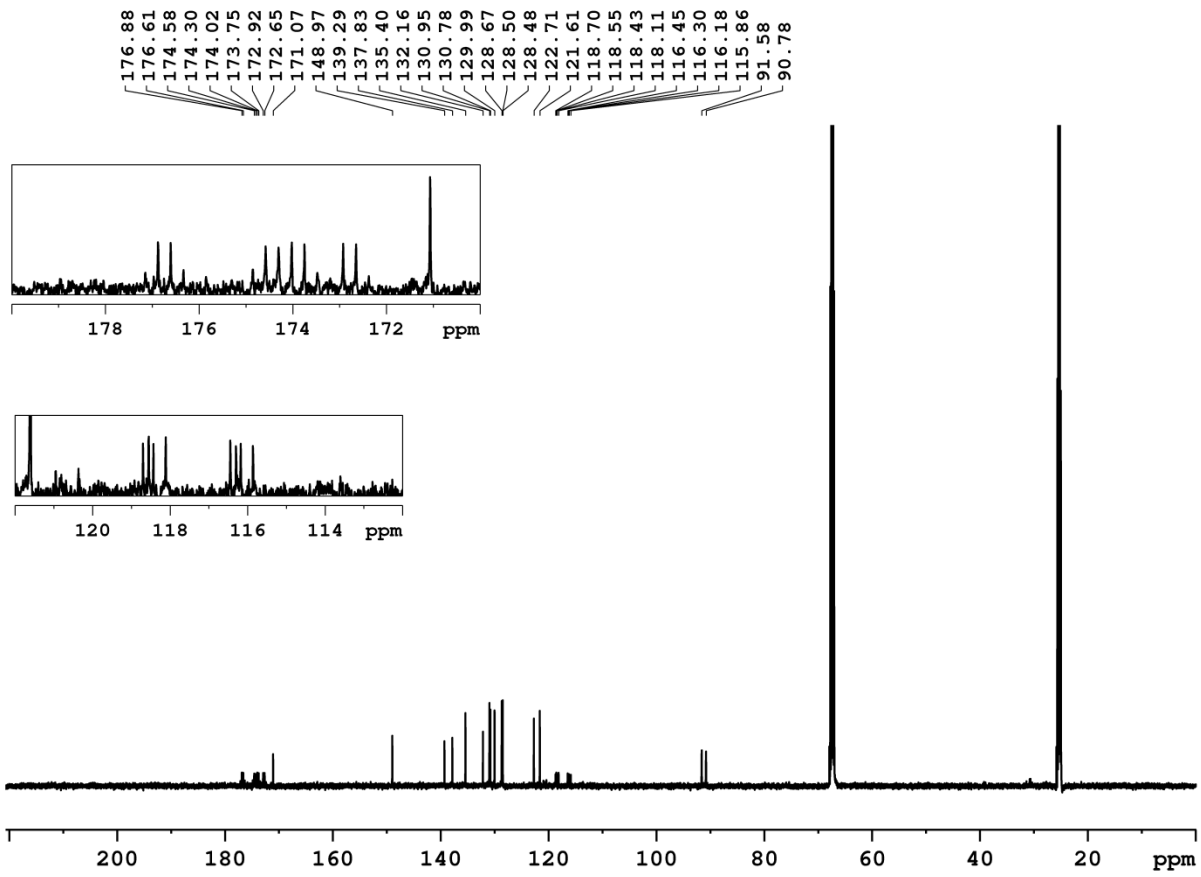

Figure S13. ^{13}C NMR (125 MHz, *d8*-THF, 298 K) spectrum of *meso* diruthenium complex **1a**.

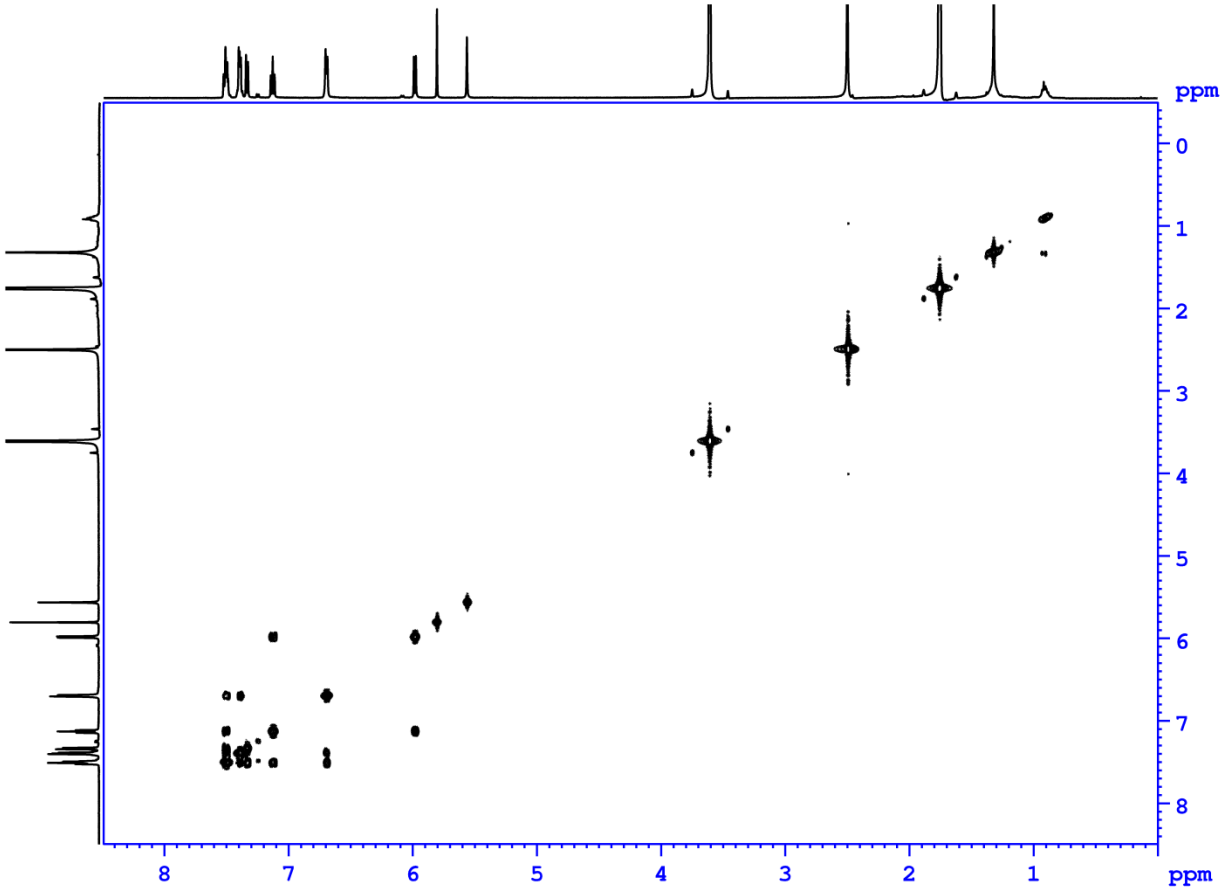

Figure S14. COSY NMR (500 MHz, *d8*-THF, 298 K) spectrum of *meso* diruthenium complex **1a**.

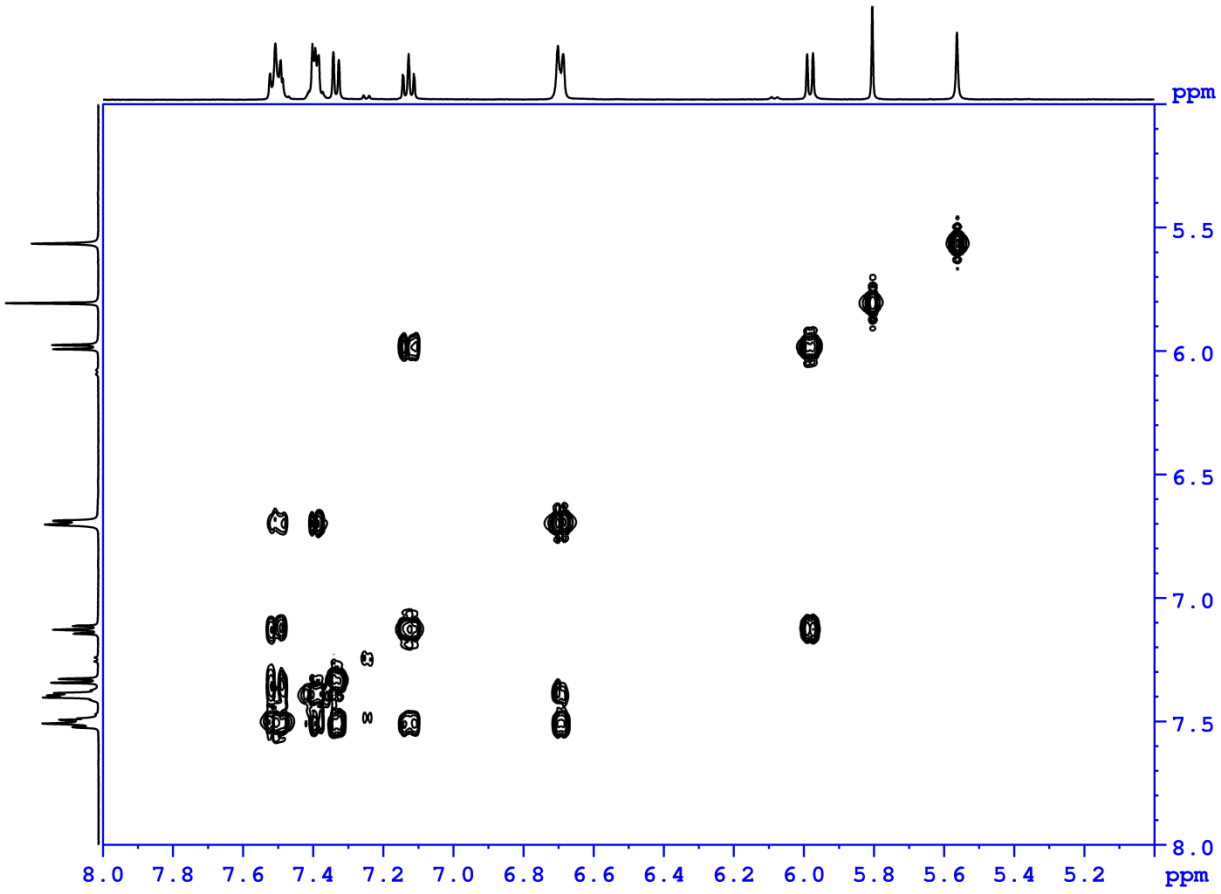

Figure S15. COSY NMR (500 MHz, *d8*-THF, 298 K) expanded spectrum of *meso* diruthenium complex **1a** showing the region 8–5ppm.

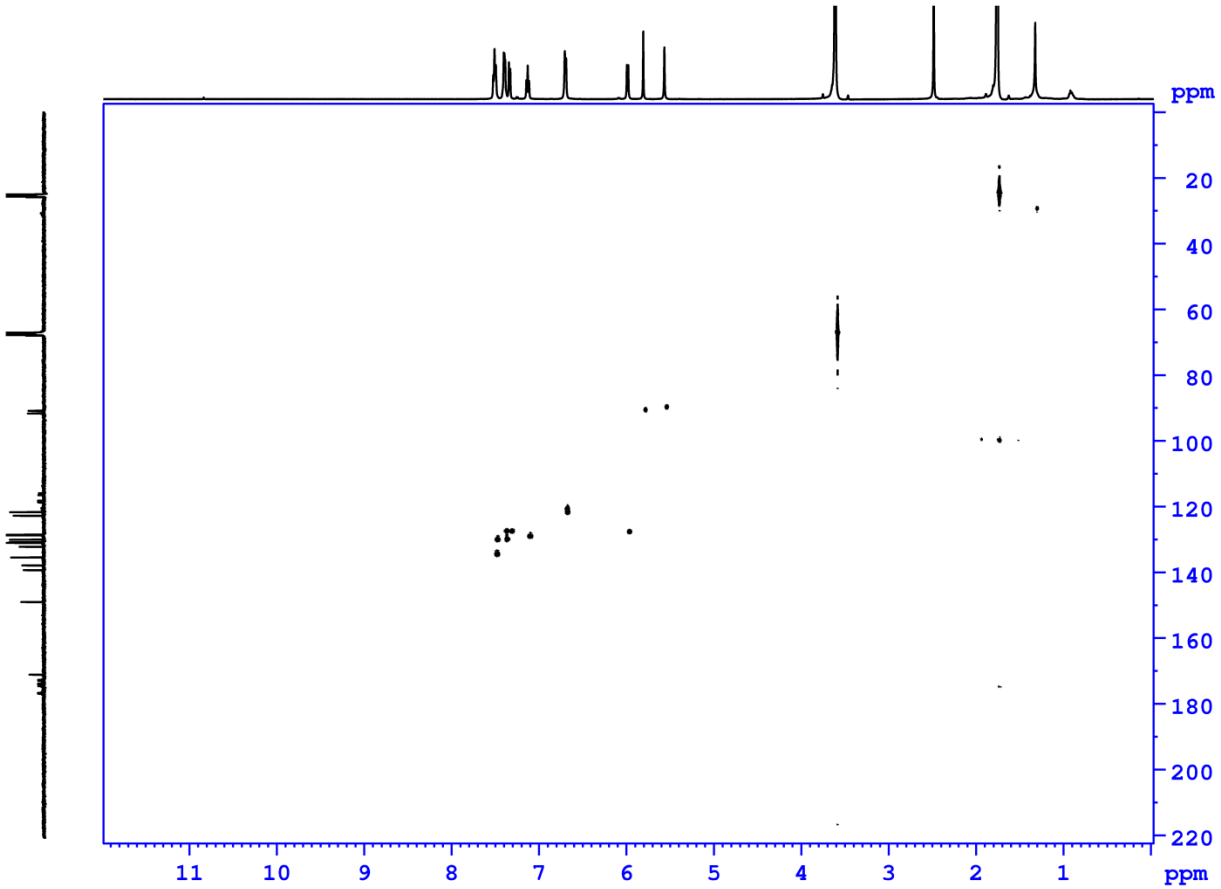

Figure S16. HSQC NMR (500 MHz, *d8*-THF, 298 K) spectrum of *meso* diruthenium complex **1a**.

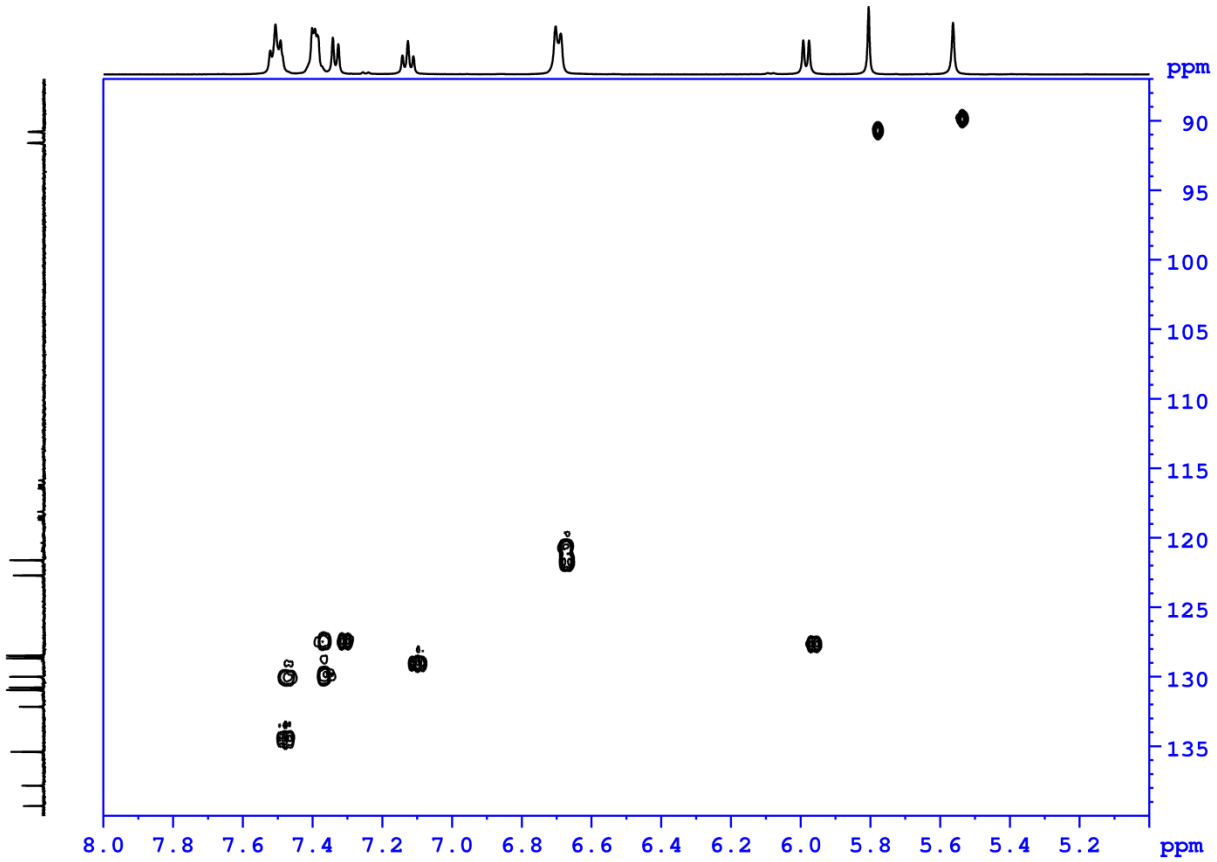

Figure S17. HSQC NMR (500 MHz, *d8*-THF, 298 K) expanded spectrum of *meso* diruthenium complex **1a** showing the region 8–5ppm and 140–87 ppm.

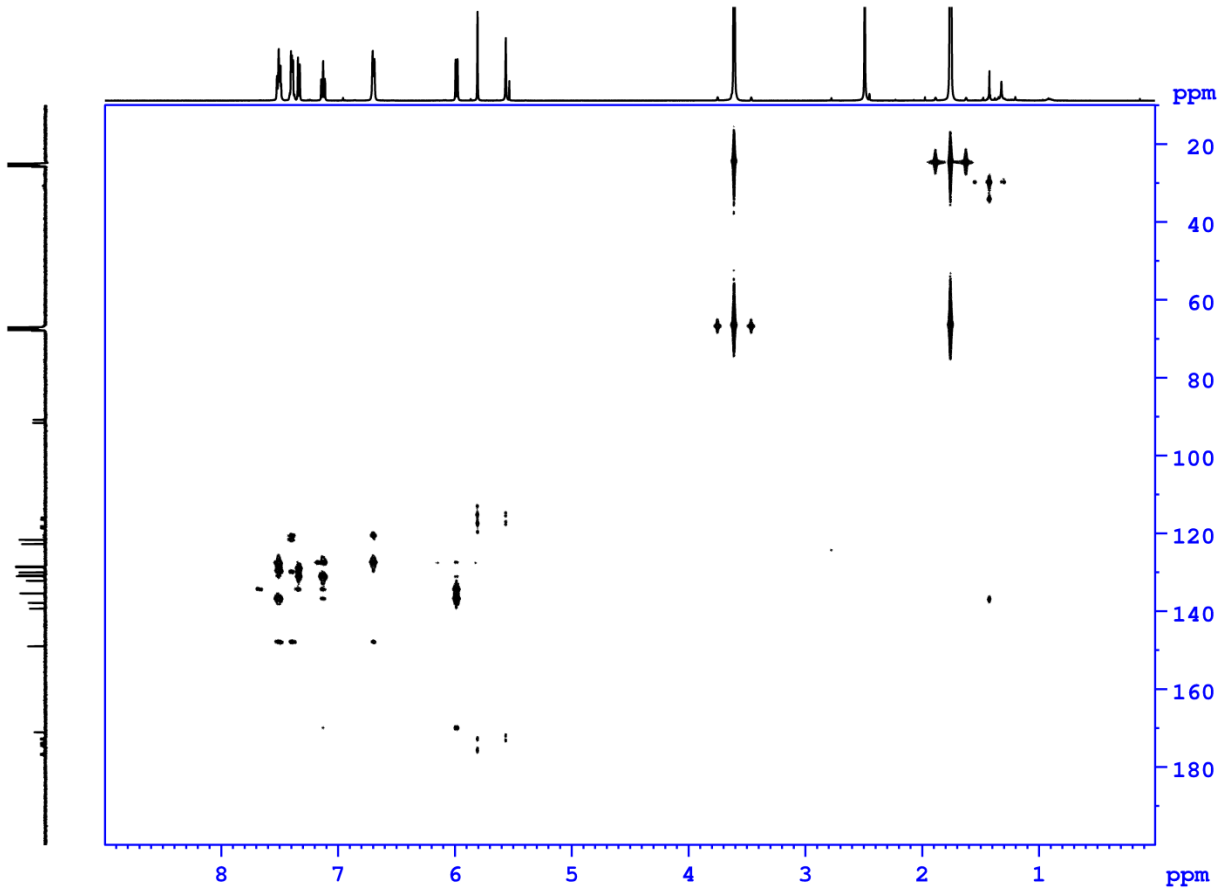

Figure S18. HMBC NMR (500 MHz, *d8*-THF, 298 K) spectrum of *meso* diruthenium complex **1a**.

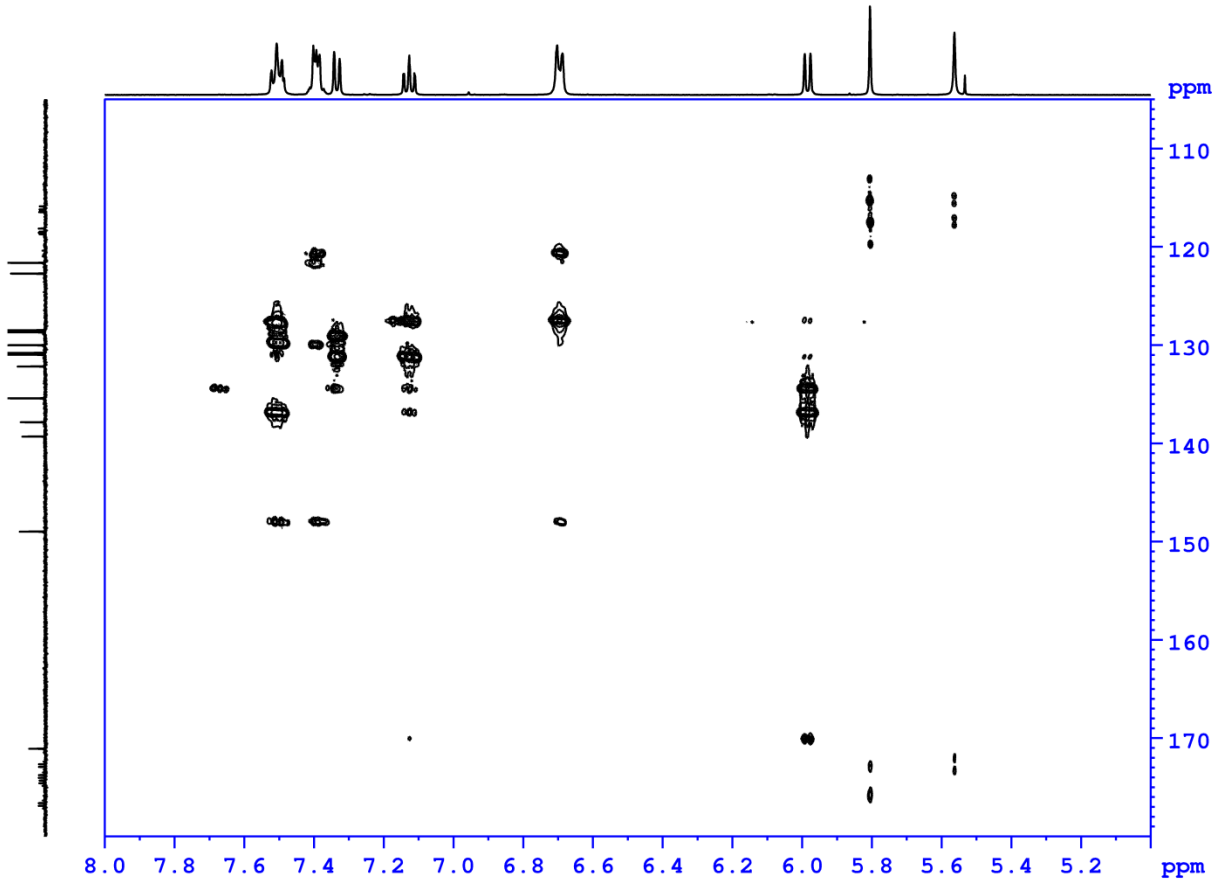

Figure S19. HMBC NMR (500 MHz, *d8*-THF, 298 K) expanded spectrum of *meso* diruthenium complex **1a** showing the region 8–5ppm and 180–105 ppm.

8. ^{1}H, ^{19}F, ^{13}C, COSY, HSQC, HMBC NMR spectra for compound **1b**

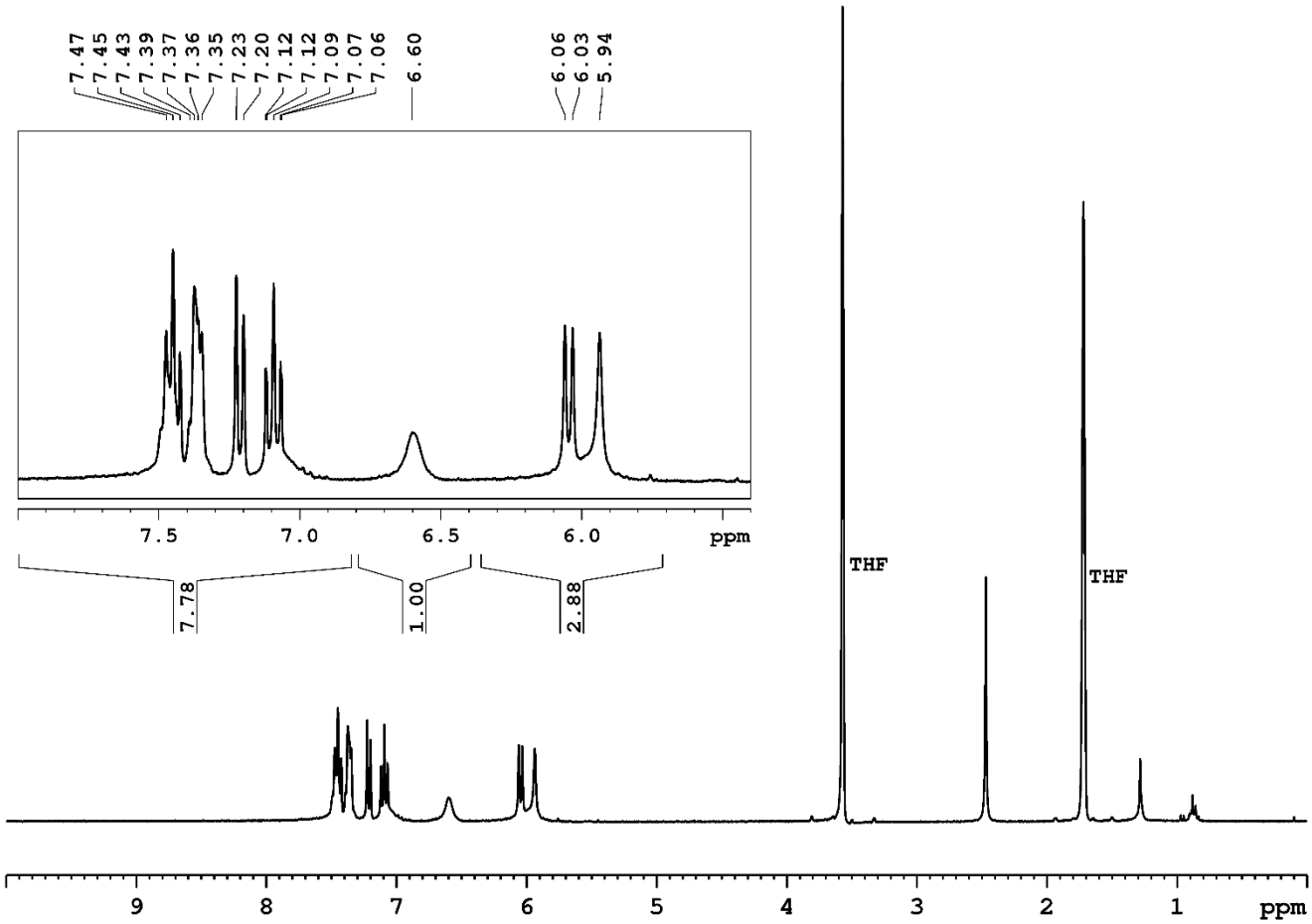

Figure S20. ^{1}H NMR (300 MHz, *d8*-THF, 298 K) spectrum of *rac* diruthenium complex **1b**.

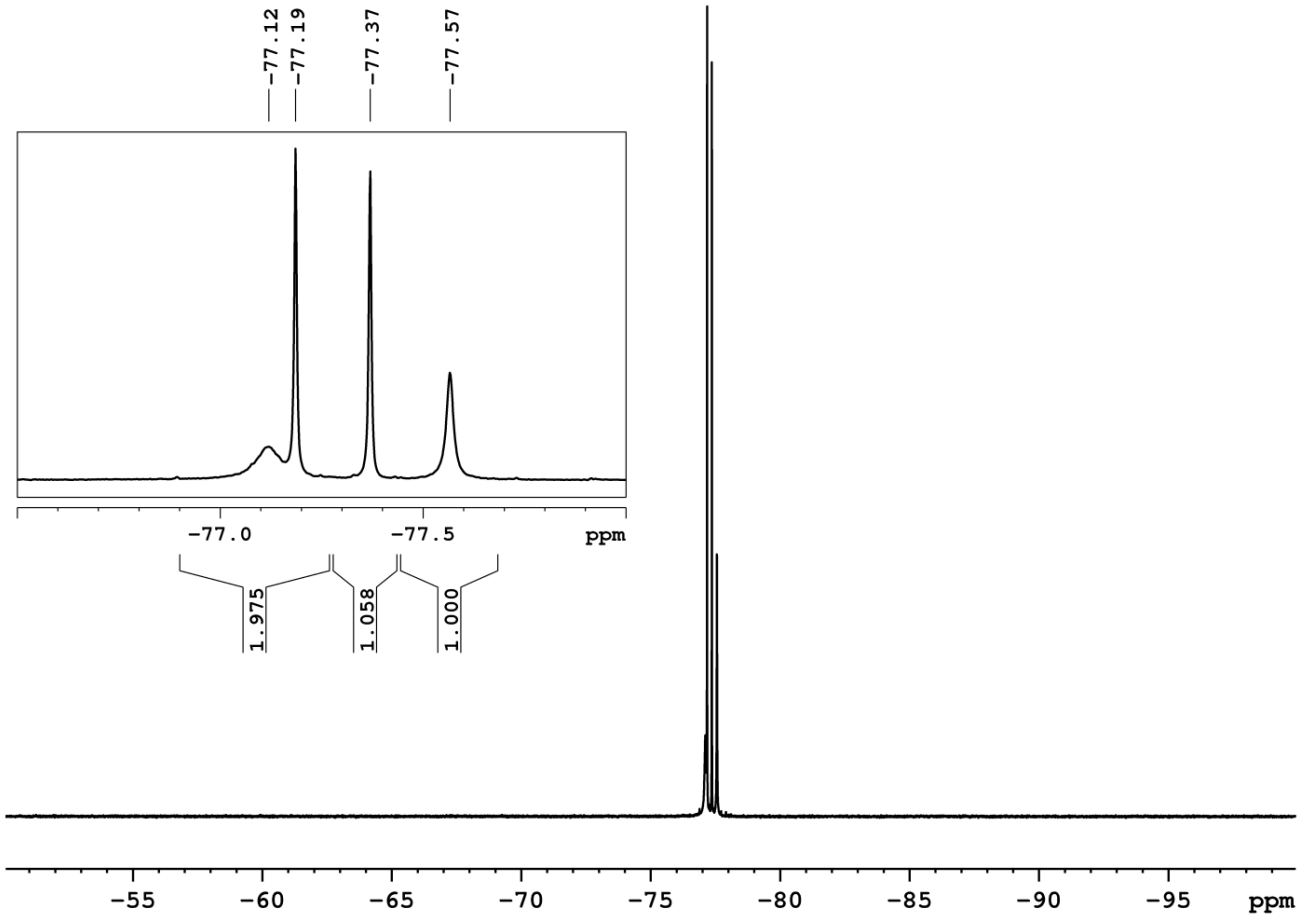

Figure S21. ^{19}F NMR (338 MHz, *d8*-THF, 298 K) spectrum of *rac* diruthenium complex **1b**.

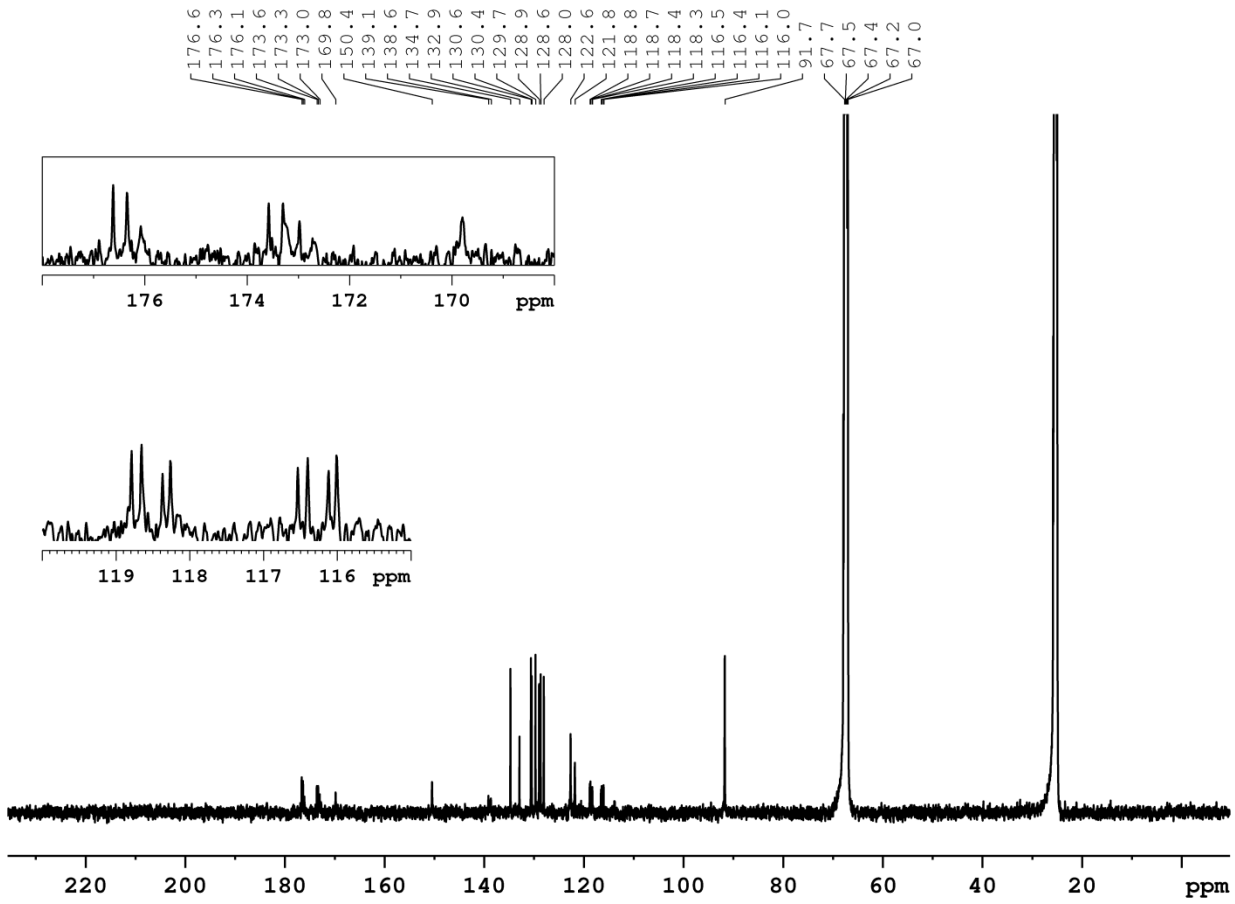

Figure S22. ^{13}C NMR (125 MHz, *d8*-THF, 333 K) spectrum of *rac* diruthenium complex **1b**.

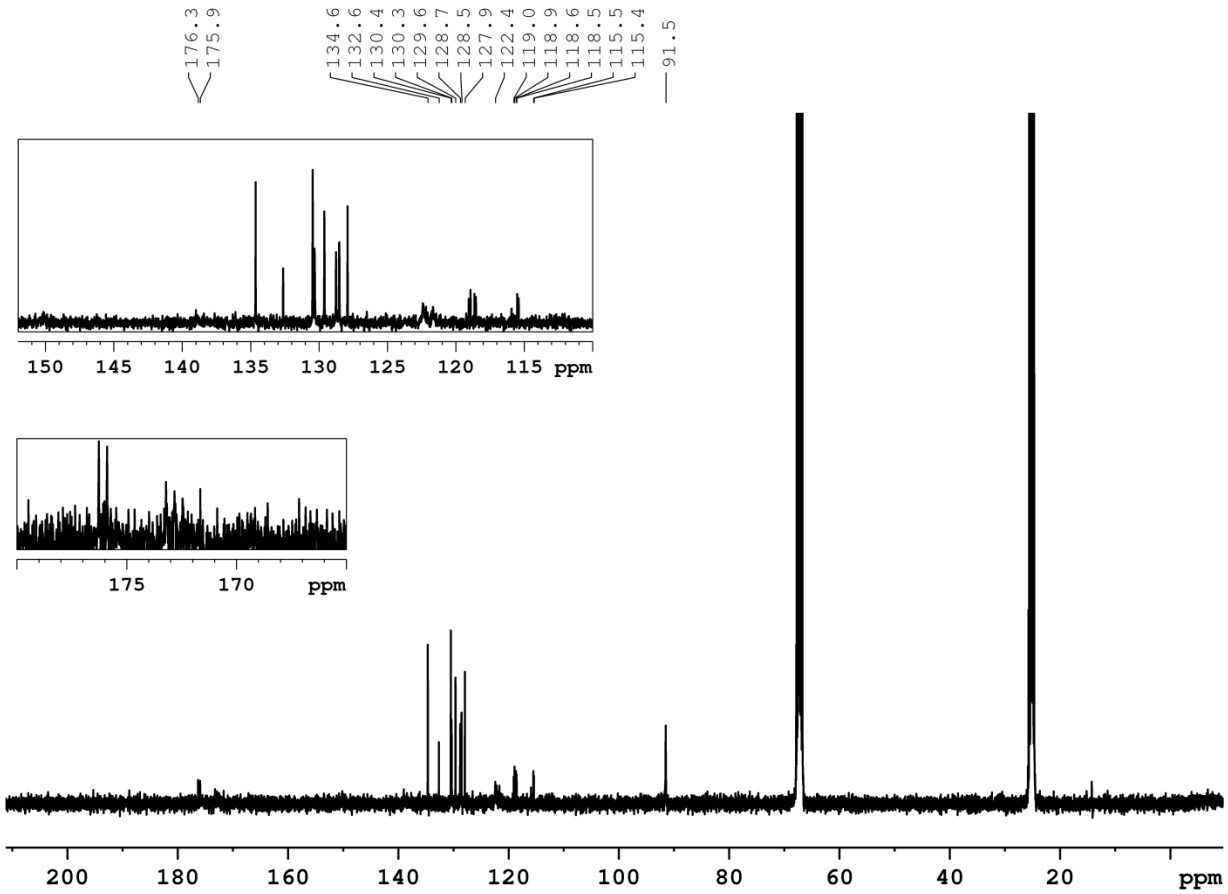

Figure S23. ^{13}C NMR (90 MHz, *d8*-THF, 298 K) spectrum of *rac* diruthenium complex **1b**.

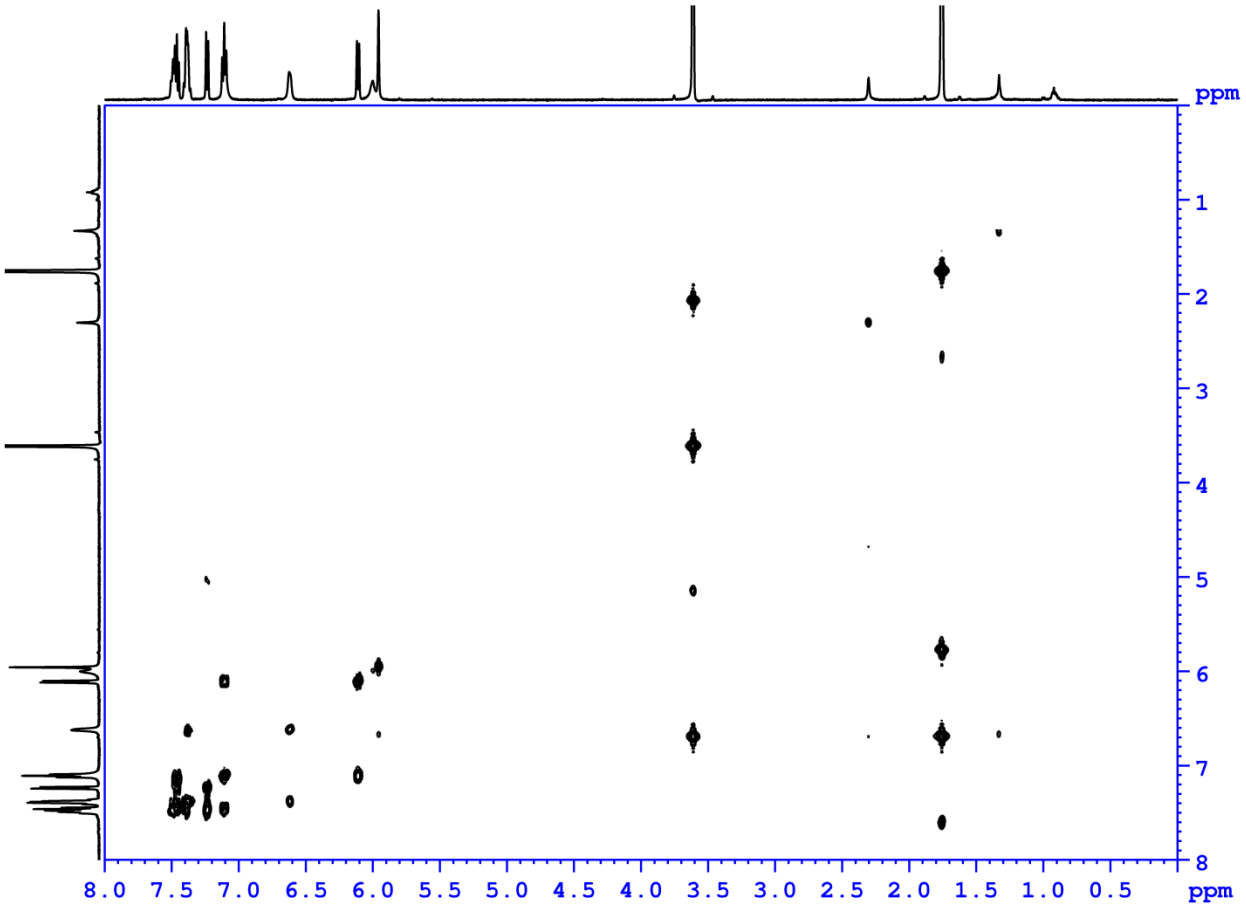

Figure S24. COSY NMR (500 MHz, *d8*-THF, 333 K) spectrum of *rac* diruthenium complex **1b**.

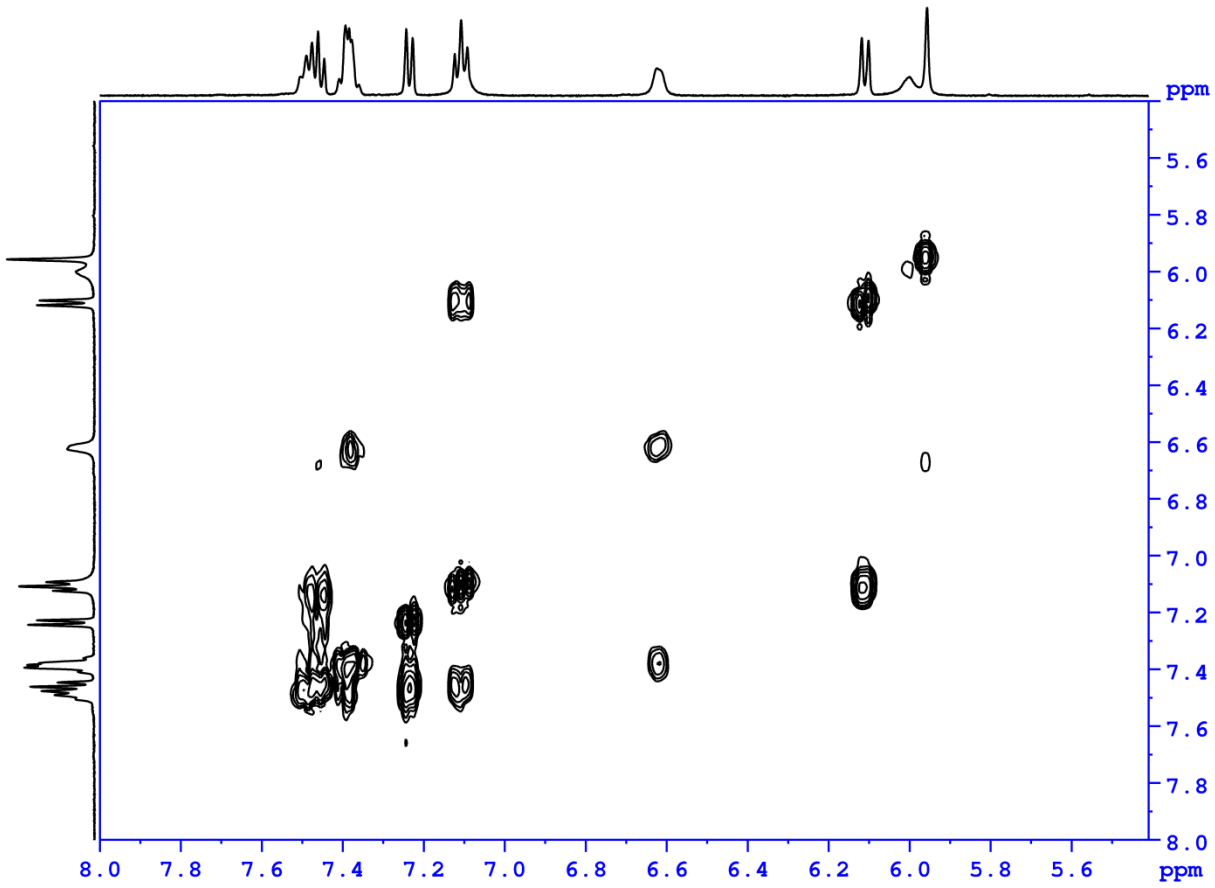

Figure S25. COSY NMR (500 MHz, *d8*-THF, 333 K) expanded spectrum of *rac* diruthenium complex **1b** showing the region 8–5.4ppm.

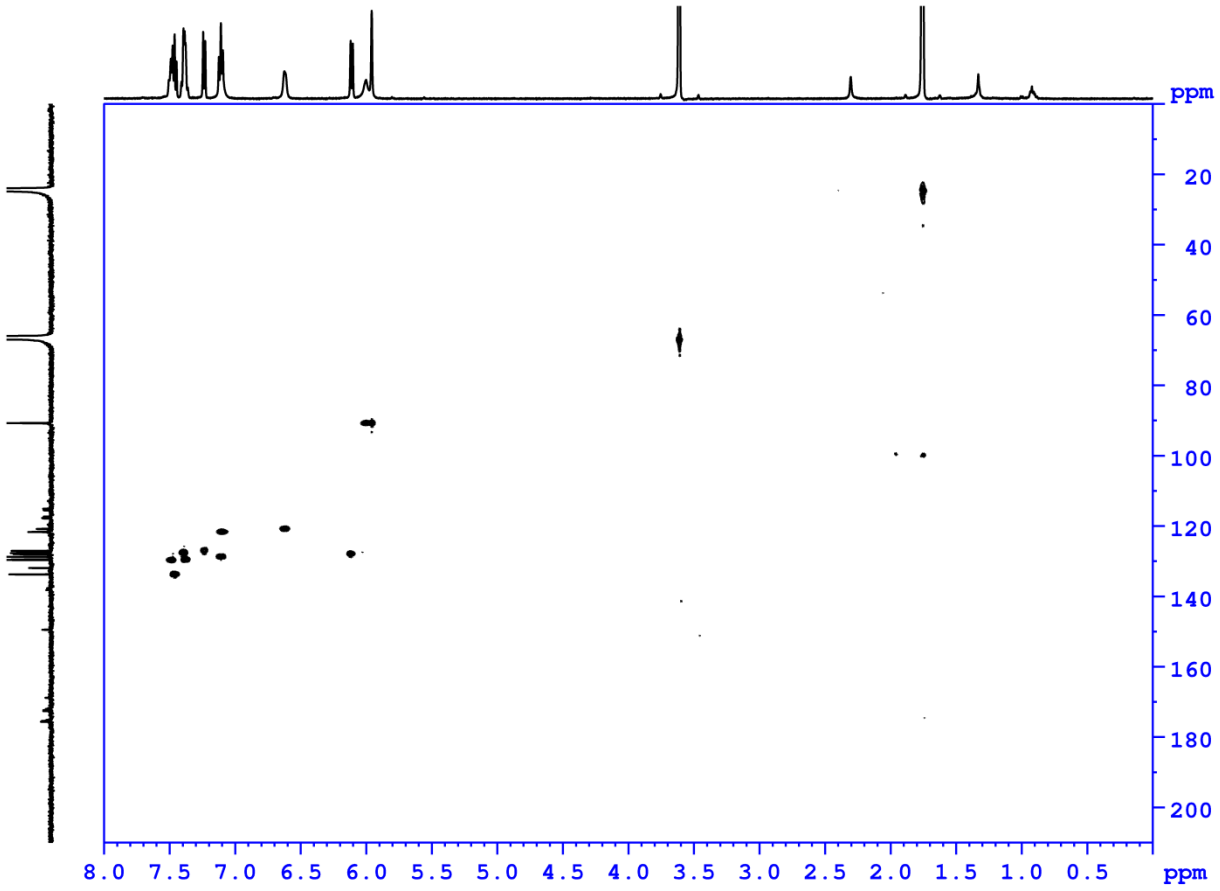

Figure S26. HSQC NMR (500 MHz, *d8*-THF, 333 K) spectrum of *rac* diruthenium complex **1b**.

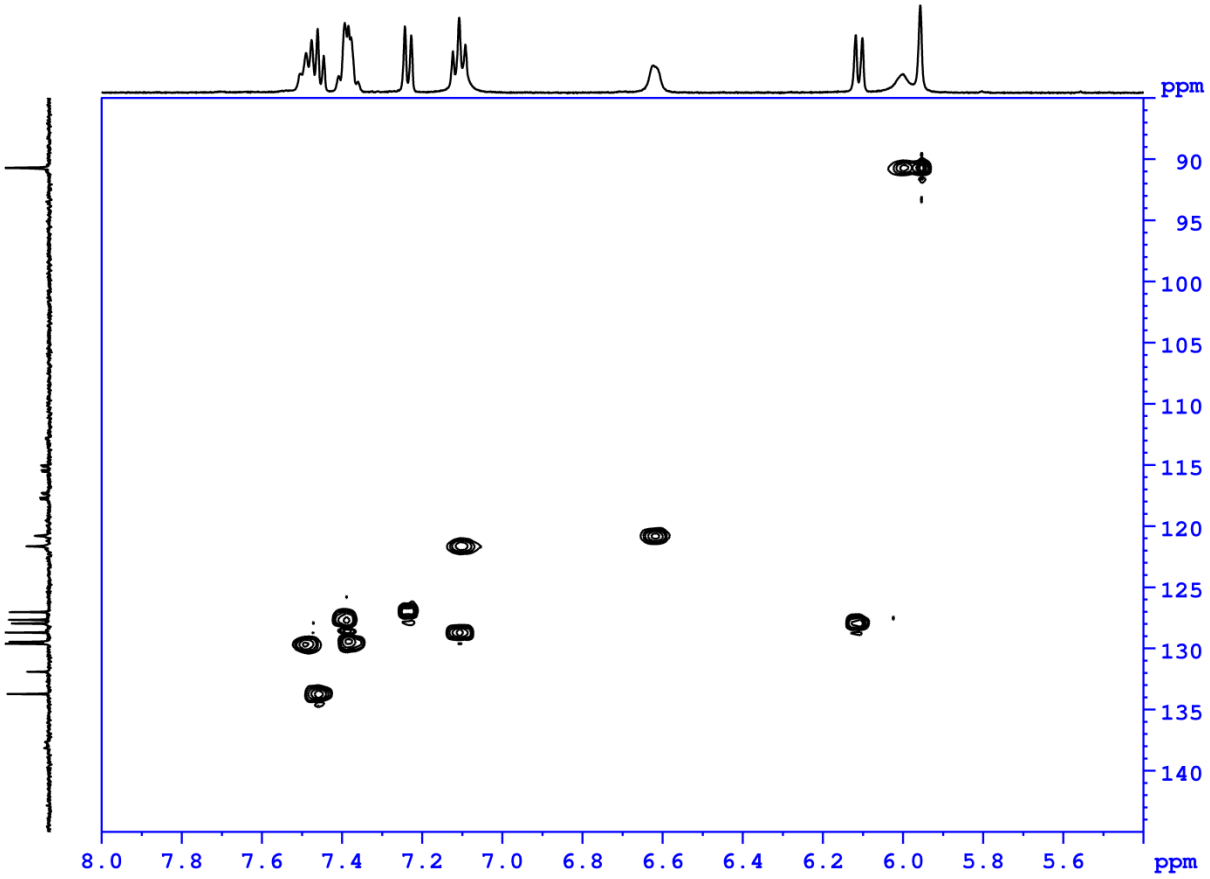

Figure S27. HSQC NMR (500 MHz, *d8*-THF, 333 K) expanded spectrum of *rac* diruthenium complex **1b** showing the region 8–5.5 ppm and 145–85 ppm.

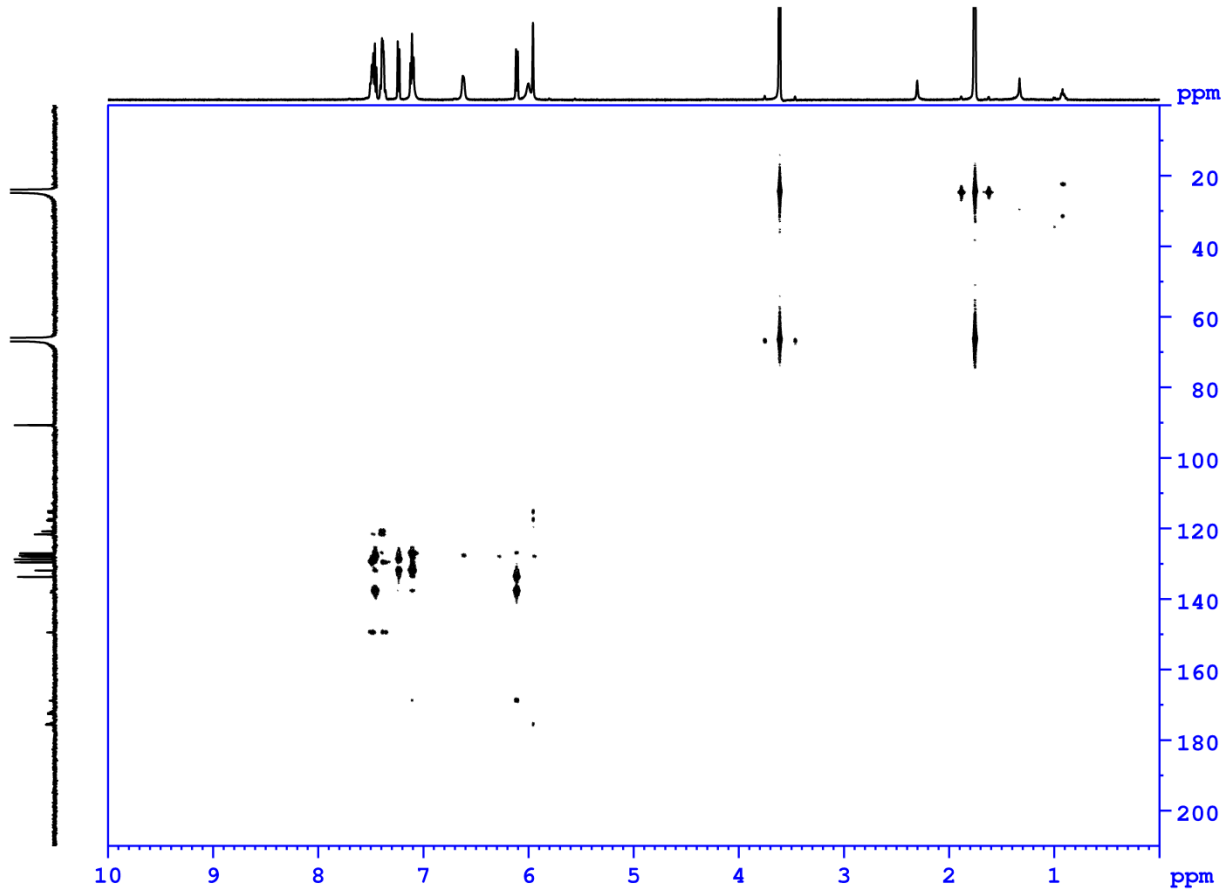

Figure S28. HMBC NMR (500 MHz, *d8*-THF, 333 K) spectrum of *rac* diruthenium complex **1b**.

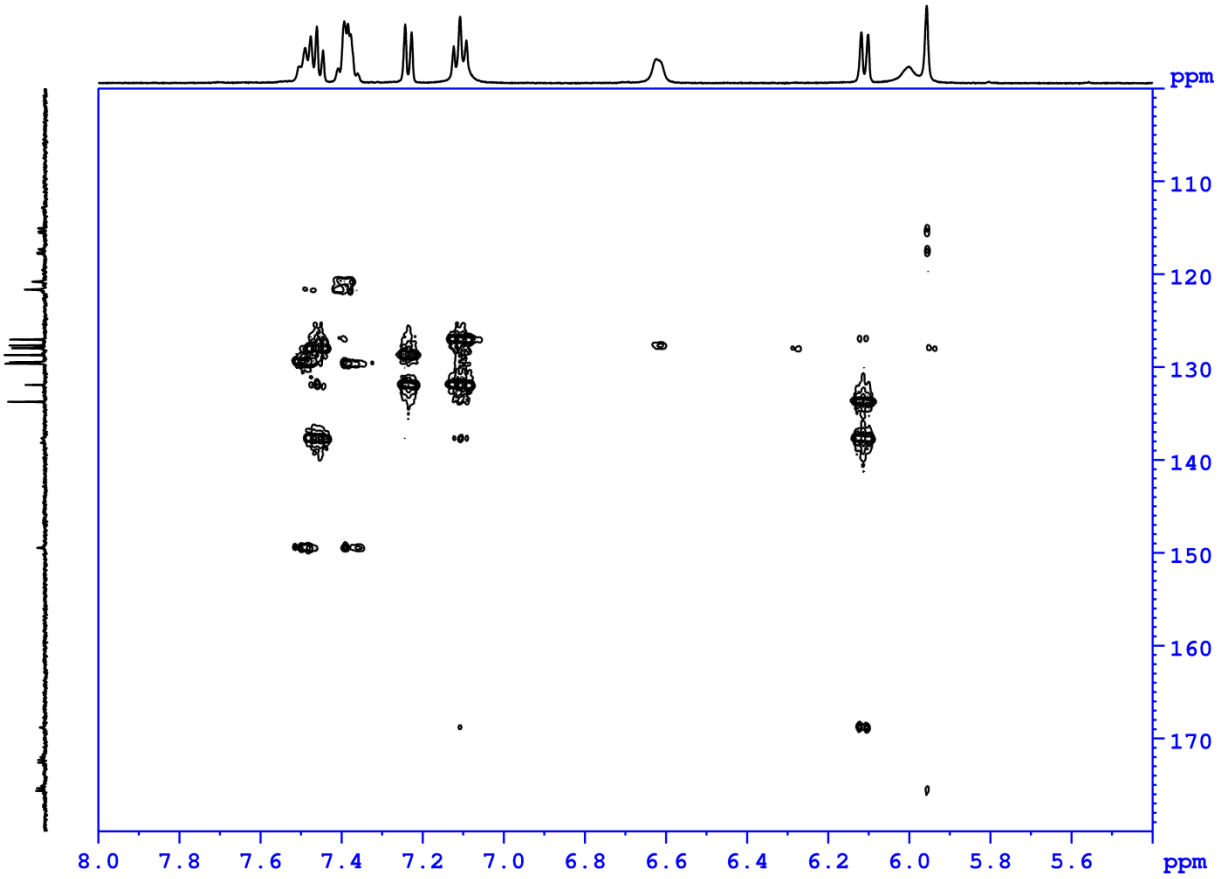

Figure S29. HMBC NMR (500 MHz, *d8*-THF, 333 K) expanded spectrum of *rac* diruthenium complex **1b** showing the region 8–5.5 ppm and 180–100 ppm.

9. ^{1}H, ^{19}F, ^{13}C NMR spectra for compound **2**.

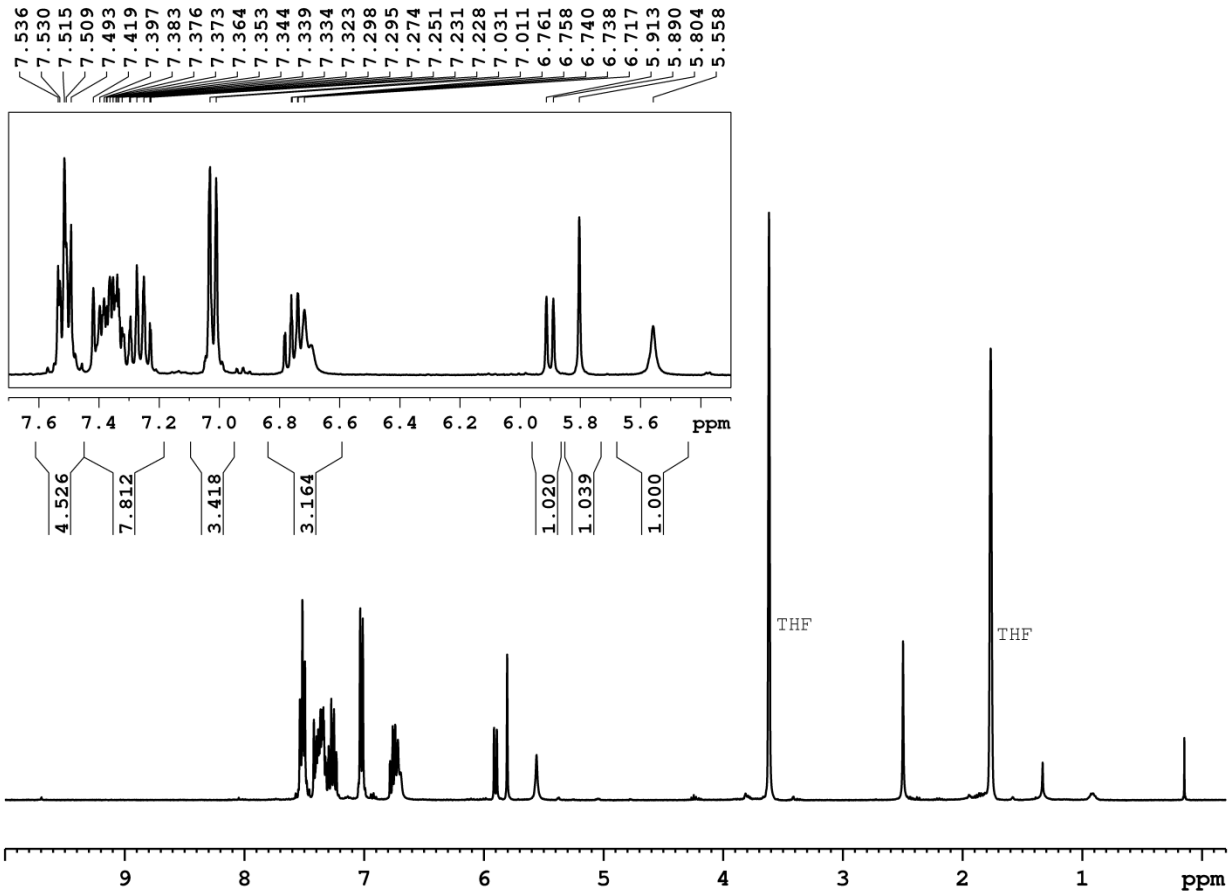

Figure S30. ^{1}H NMR (360 MHz, *d8*-THF, 298 K) spectrum of monoruthenium complex **2**.

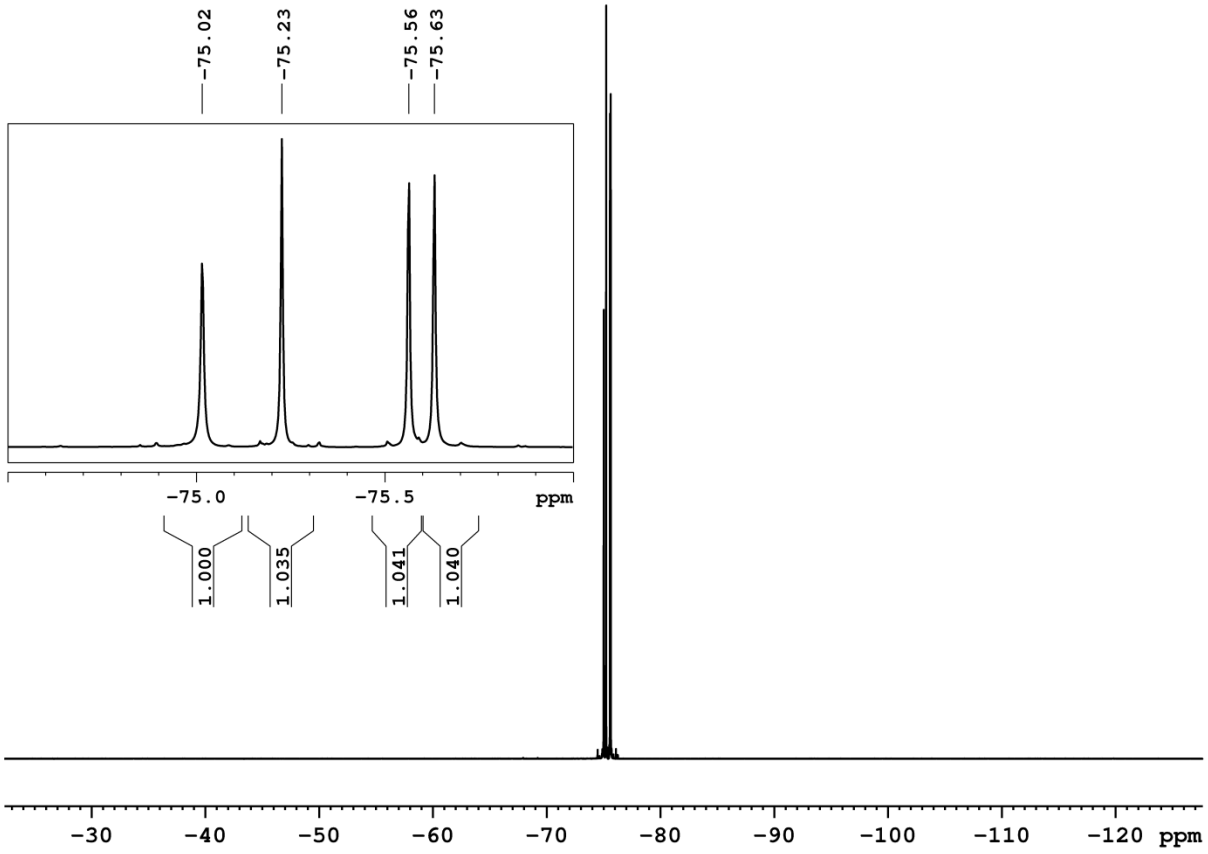

Figure S31. ^{19}F NMR (282 MHz, *d8*-THF, 298 K) spectrum of monoruthenium complex **2**.

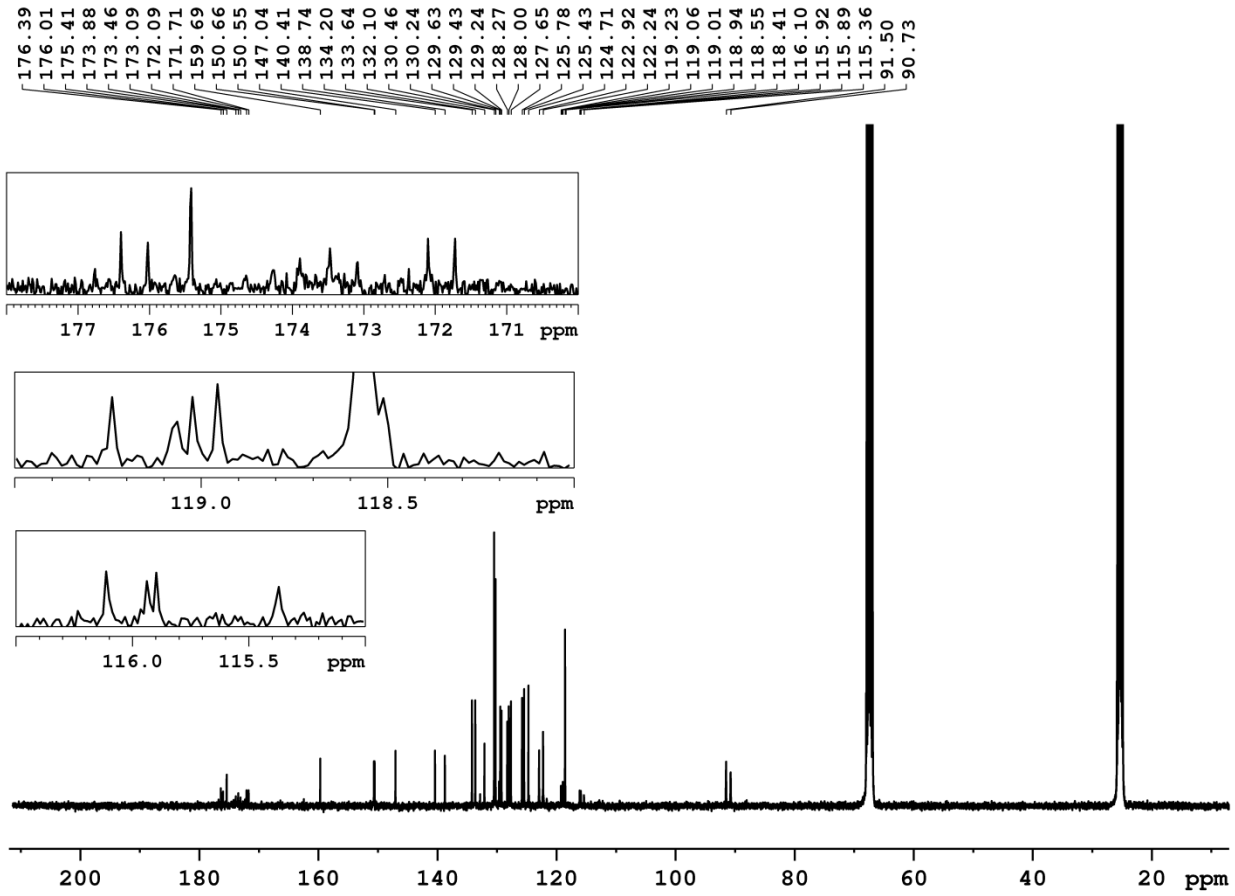

Figure S32. ^{13}C NMR (90 MHz, *d8*-THF, 298 K) spectrum of monoruthenium complex **2**.

10. Variable temperature ^{1}H NMR spectra of *rac* diruthenium **1b**, winDNMR simulations, and $\Delta G^{\ddagger}$ calculations.

^{1}H NMR spectra of **1b** at varied temperatures were collected in d8-THF at 500 MHz. Line shape analysis of these spectra was performed using winDNMR Pro 7.1. The spectra show a large number of exchanging signals with large differences in chemical shift between the conformers. Because of this, it was not possible to find a spectral window that contained

isolated exchanging signals throughout the 208 – 331 K temperature range. A simulation using the two pairs of coalescing singlets generated by the Hfac protons (a 2 x 2 spin simulation in winDNMR) was therefore deemed the best choice. The positions of the two pairs of coalescing singlets at 208 K are: 6.59 ppm/~5.6 ppm (3284 Hz and 2796 Hz) and 6.23 ppm/5.83 ppm (3120 Hz and 2926 Hz). The spectral range examined for line shape analysis was 6.7 – 5.4 ppm.

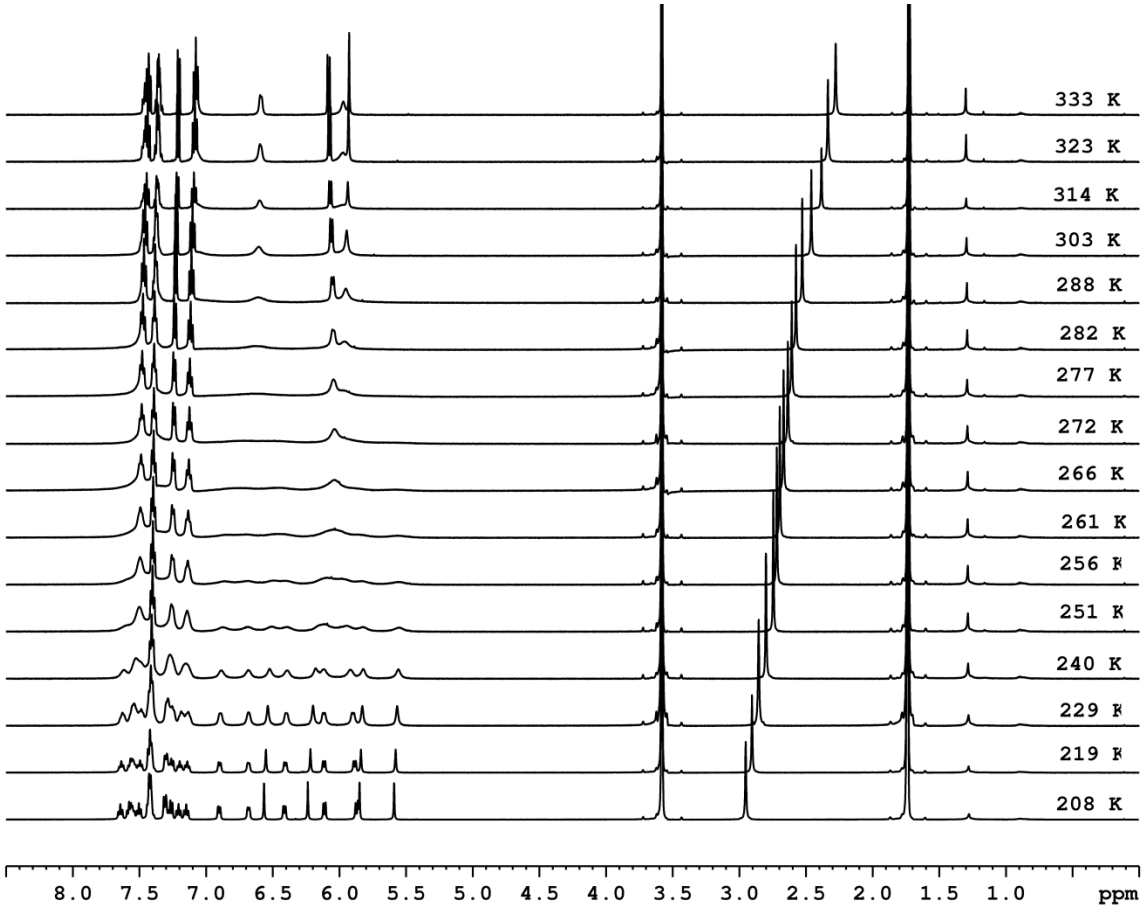

Figure S33. Variable temperature ^{1}H NMR spectra (d8-THF, 500 MHz) for *rac* diruthenium complex **1b**.

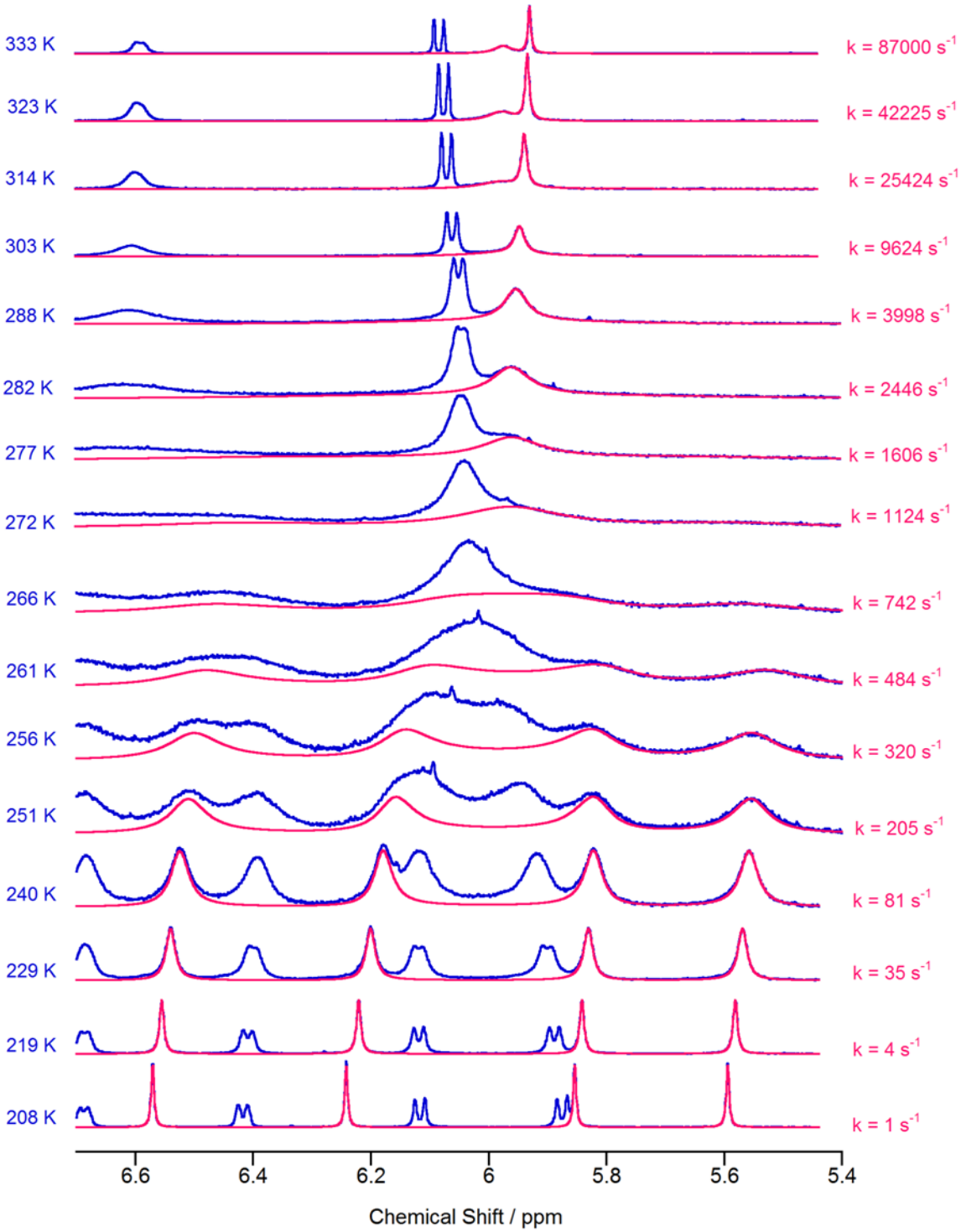

Figure S34. Variable temperature ^{1}H NMR spectra (blue) and winDNMR simulations (red) for *rac* diruthenium complex **1b**. The temperatures of the spectra and the rate constants obtained for the corresponding simulations are indicated in the figure.

A standard Eyring plot of ln(k/T) versus 1/T was used to determine activation parameters for the conformational exchange. The slope of the graph was used to calculate the enthalpy of activation using equation (1) where R is the gas constant 1.9872 calories mol^{-1}.

$$\Delta H^{\ddagger} = -slope \times R \quad (1)$$

The entropy of activation was calculated with equation (2) using the intercept of the plot, where k_b is the Boltzmann constant, h is Planck's constant, and R is the gas constant 1.9872 calories mol^{-1}.

$$\Delta S^{\ddagger} = (Intercept - \ln(k_b/h)) \times R \quad (2)$$

The Gibbs free energy of activation at 298 K was calculated from the enthalpy and entropy of activation using equation (3)

$$\Delta G^{\ddagger} = \Delta H^{\ddagger} - T\Delta S^{\ddagger} \quad (3)$$

The rate constant k at 298 K was obtained using the line fit from the Eyring plot, rearranged in equation (4).

$$k = e^{((-5804.6/T) + 22.85 + \ln T)} \quad (4)$$

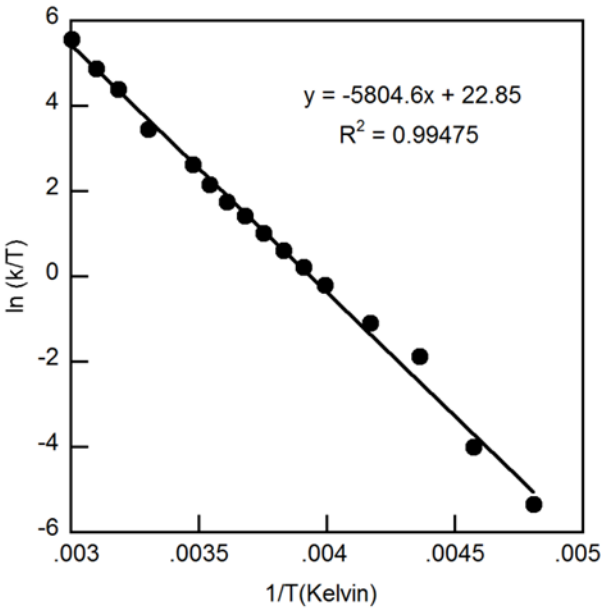

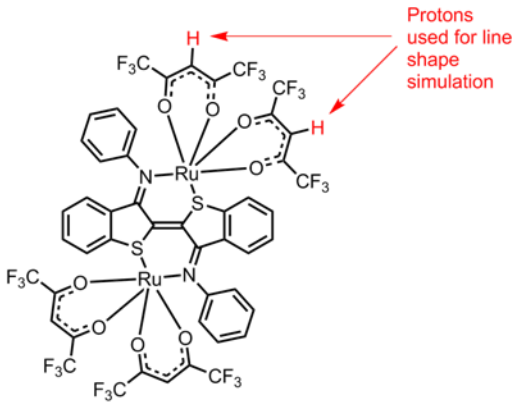

$\Delta H^{\ddagger} = 11.5$ kcal mol^{-1}
$\Delta S^{\ddagger} = -1.8$ cal mol^{-1} K^{-1}
$\Delta G^{\ddagger}_{298} = 12.0$ kcal mol^{-1}

Figure S35. Eyring plot (left) using data from the variable temperature spectra and simulations of **1b** shown in figure S34 above. The structure of **1b** (right) showing the protons used for the line shape analysis.

11. Low temperature ^{19}F spectra for compounds **1a** and **1b** and low temperature ^{1}H NMR spectra for compound **1a**.

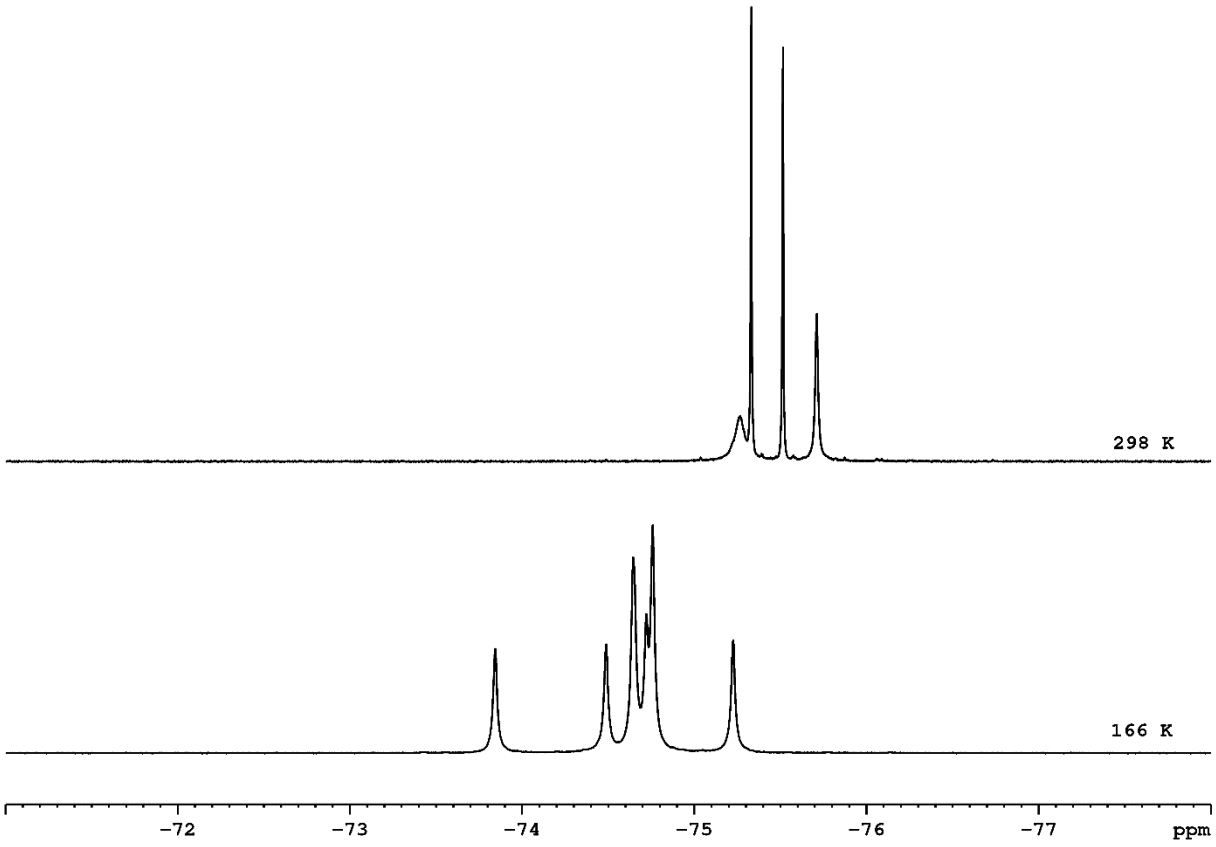

Figure S36. Variable temperature ^{19}F NMR spectra of *rac* diruthenium **1b** (338 MHz, d8-THF) showing the effects of temperature-dependent rates of conformational exchange at 298 K and 166 K. The resolved peaks of the two conformers are seen at 166 K. Broadening and coalescence of these peaks is evident at 298 K.

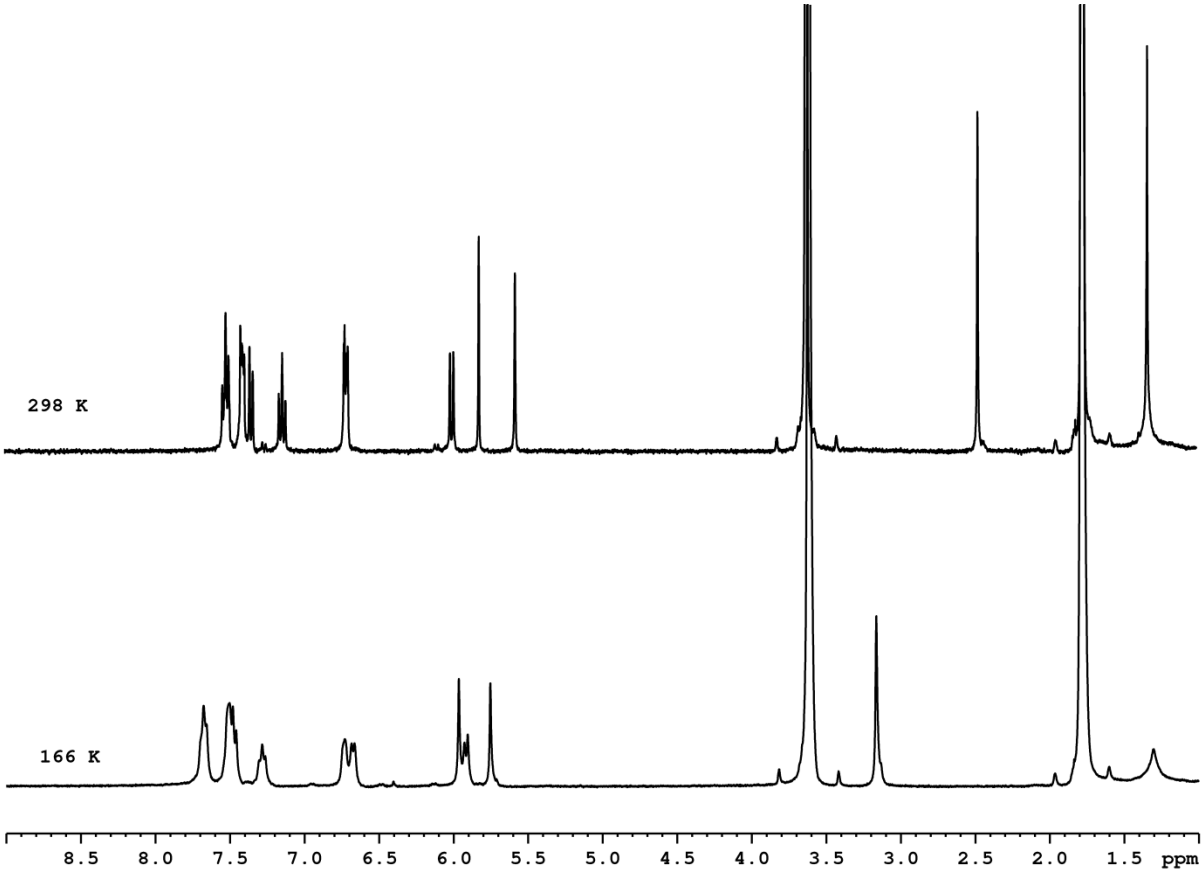

Figure S37. Variable temperature ^{1}H NMR spectra of *meso* diruthenium **1a** (360 MHz, d8-THF). The spectra do not show any evidence of dynamic exchange at 298 or 166 K.

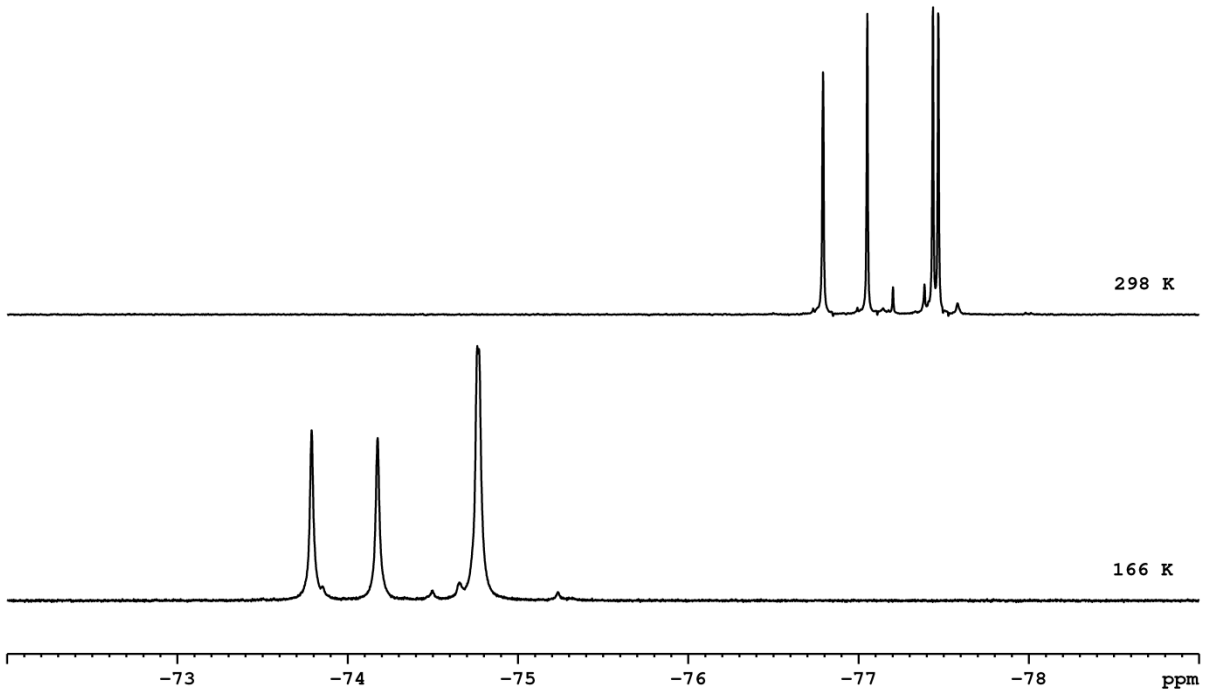

Figure S38. Variable temperature ^{19}F NMR spectra of *meso* diruthenium **1a** (338 MHz, d8-THF). The spectra do not show any evidence of dynamic exchange at 298 or 166 K.